Bioorganic Chemistry xxx (xxxx) xxx

Contents lists available at ScienceDirect

Bioorganic Chemistry

journal homepage: www.elsevier.com/locate/bioorg

Design, synthesis of Cinnamyl-paeonol derivatives with 1, 3-Dioxypropyl as link arm and screening of tyrosinase inhibition activity *in vitro*

Kai Tang [1], Yi Jiang [1], Huawei Zhang, Wenli Huang, Yundong Xie, Chong Deng [*], Hongbo Xu, Xiaomei Song, Hong Xu

Shaanxi University of Chinese Medicine, Xianyang 712046, China

ARTICLE INFO

Keywords:
Cinnamic acid
Peaonol
Tyrosinase inhibitors
Anti-melanin
Molecular docking

ABSTRACT

This study aimed to obtain tyrosinase inhibitors for treating hyperpigmentation. A series of cinnamyl ester analogues were designed and synthesized with cinnamic acid (CA) and peaonol compounds. The safety, melanin content and inhibitory effects of all target compounds were evaluated. In the enzymatic activity test, the inhibitory rate of compounds 8, 13 and 14 had stronger inhibitory activity with the IC_{50} values of 20.7 μM, 13.98 μM and 15.16 μM, respectively than the positive drug kojic acid (IC_{50} with 30.83 μM). The cytotoxicity evaluation showed that compounds 13 and 14 have higher safety than the other compounds to the proliferation of B16F10 cells. The result of the melanocyte test supported that compound13 has stronger cellular tyrosinase inhibitory activity than kojic acid and arbutin at 100 μM and 200 μM. The enzyme kinetics mechanism revealed that compound 13 was a non-competitive inhibitor while compounds 8 and 14 were mixed inhibitors. For the experiments of melanin content and tyrosinase activity in the B16F10 melanona cells, the inhibition rates of compounds 8, 14 and 13 were with 19.62%, 20.59% and 23.83%, respectively. In addition, compound 13 revealed the highest inhibitory activity to tyrosinase in the melanocyte with inhibition rates of 23.83%, which was better than kojic acid and arbutin (19.21% and 20.45%) at the same concentration. In the anti-melanogenesis experiment, compounds 8 and 13 had better anti-melanin effects than kojic acid from 25 μM to 100 μM. In summary, the results indicated that compounds 8, 13 and 14 had better tyrosinase inhibitory activity and anti-melanogenesis activity. Especially, the compound 13 has potentiality to develop novel tyrosinase inhibitors and whitening agents. The docking studies results revealed that the functional group of compound 13 mostly depends on the phenolic hydroxyl moiety, and its hydroxyl group did not insert into the active site of tyrosinase, which was in agreement with the results of the kinetics study.

1. Introduction

Tyrosinase, as a multifunctional copper-containing oxidase, is widely scattering in plants, animals and microorganisms innature, which belongs to the type 3 copper protein family [1,2]. It is also a polyphenol oxidase, containing two copper atom located in the active site. The activation of tyrosinase is closely related to the rate of melanogenesis [3]. Melanin, one of the most widely distributed pigments in nature, is responsible for color of human skin, animal fur and plant browning. Tyrosinases, tyrosinase-related protein 1(TRP-1) and tyrosinase-related protein 2(TRP-2), are well-known melanogenic limited enzymes, which play an essential role in the regulation of melanogenesis. Among of them, tyrosinase is the most important factor to regulate melanogenesis [4], which catalyze biosynthesis of melanin involved in two different reactions [5] including from hydroxylation of monophenols to o-diphenols and oxidation of o-diphenols to the corresponding o-quinones [6]. In addition, the process of melanogenesis is confined to special melanosomes in melanocytes, which synthesize pigments and transfer them to the recipient cells. Eventually, a series of highly reactive quinones prompt melaniogenesis, which is responsible for melanin of the skin, hair and eyes. In conclusion, melaninis produced from oxidation and polymerization of tyrosinase and plays irreplaceablevital role in normal function of bioorganism [7–9]. However, excessive production of melanin results in some pigmentation disorders, such as melanoma, melasma, frecklesand post-inflammatory hyperpigmentation. Especially, melanoma is a form of skin cancer that arises from the aberrant

* Corresponding author.
E-mail address: 2051079@sntcm.edu.cn (C. Deng).
[1] Kai Tang, Yi Jiang contributed equally to this work.

https://doi.org/10.1016/j.bioorg.2020.104512
Received 9 August 2020; Received in revised form 10 October 2020; Accepted 19 November 2020
Available online 24 November 2020

proliferation of melanocyte [10–13]. Furthermore, recent studies reported that melanin involved in the substantianigra(SN) of humans contributing to an important role in the brain neuromelanin development, such as parkinson and other degenerative diseases [14–16]. Therefore, controlling a tyrosinase-dependent mechanism of melanogenesis might be the basis for a potential anti-melanoma therapy, and inhibition of melanogenesis is one of reasonable method to cure hyperpigmentation. As an essential and rate-limiting enzyme to regulate melanogenesis, excessive activation of tyrosinase causes various dermatological disorders. Hence, tyrosinase has been seen asan important target for developing therapeutic agents of pigment disorders. Tyrosinase inhibitors have been increasingly attention from researchers to prevent or treat pigmentation disorders. In recent years, many articles reported that a series of natural and synthesized products had inhibitory activity of tyrosinase and anti-melaninogenic, such as vinca major and its secondary metabolite [17,18], N-(4-methoxyphenyl)caffeic amide [19], 3-heteroarylcoumarins [20], flavonoids [21], cinnamic acid ester derivatives [22], 3-heteroarylcoumarins [23], carvacrol derivatives [24],flavones [25],substituted vanllylcinnamate, and so on [26,27].

However, some well-knowninhibitors: kojicacid [28], azelaic acid [29,30], arbutin [31], tropolone and hydroquinone [32,33]were limited in medicine and cosmetics industry because of the side-effect such as cytotoxicity, skin cancer, dermatitis and neurodegenerative disease [2,20,28–34]. Therefore, those problems prompt us to search for safer, more effective and cheaper tyrosinase inhibitors. Especially natural products existed in Chinese medicinehas been increasingly paying attention to researchers on account of low cytotoxicity and tyrosinase inhibitory activity, such as caffeic acid and peaonol derivatives [21,22,35,36], the structure of those compounds was showed Fig. 1. In addition, paeonol and eugenolanaloges, a type of traditional skin-whitening agent [37–39], have moderate activity on the browning and relevant enzymes of fresh-cut lettuce [40,41]. To search safer, more effective and cheaper tyrosinase inhibitors, caffeic acid derivatives were coupled with paeonol analoges by esterification reaction, which was widely applied to synthesis drugs and food additive [22,42–45].

In this study, 14 cinnamic-paeonol ester analogues were synthesized via esterification reaction with caffeic acid derivatives and paeonol analogues. The inhibitory activity and kinetic parameters of all target compounds were calculated by mushroom tyrosinase tests and the compound 8, 13 and 14 were screened out preliminary. Secondly, the safety, anti-melanogenesis activity and cell tyrosinase inhibitory effects of compound 8, 13 and 14 were estimated with murine melanoma cell line (B16F10). Finally, computational analysis was carried out the interactions with the catalytic binding site between inhibitors and amino acid residue. We hope this study could pave the way for developing novel effective tyrosinase inhibitors, searching for new whitening agents and anti-browning agents for food products and medical industry.

2. Results and discussion

2.1. Synthetic procedures

Using caffeic acid analogues (d-f) as starting materials, the two synthetic routes of the cinnamic acid ester derivatives have been showed in scheme 1. Firstly, in order to successful link the cinnamic acid derivative to the phenolic components to gain cinnamic acid esters structure, peaonol derivatives(a-c) have been etherified through Williamson reaction to ascend the activity of reaction. In spite of the phenolic hydroxyl group in the two series components has a significant influence on the subsequent reaction. Therefore, two synthetic routes were designed to synthesis target compounds 1–1 shown in Scheme 2 and in Scheme 3.

Route 1: On the one hand, acetic anhydride was used to acetylate the phenolic hydroxyl group in cinnamic acid derivatives d-f, and then $SOCl_2$ was used to make the acid chloride to enhance reaction activity; on the other hand, 3-Bromo-1-propanol and phenolic derivatives were used to synthesize ester products by Williamson reaction, finally two kinds of compounds were linked to get twin drugs through esterification reaction. Cinnamic acid analogues and peaonol derivatives were used as raw materials to synthesize compounds 1–9 with triethylamin as catalyst. Using the cinnamic acid derivatives 4e as starting material, compounds 13 and 14 were obtained by the esterification.

Route 2: TBDMSCl was used to protect the hydroxyl group in ferulic acid under alkaline conditions to obtain 4e; then compound 4e reacted with $SOCl_2$ to produce the acyl chloride, which was mixed with paeonol analogues to produces esters 10–12. Finally, TBDMS group was removed from compounds 10 and 11 by Tetrabutylammonium fluride(1.0 mol/L in THF solution) to get the target compounds 13 or 14 as shown in Scheme 3.

2.2. Mushroom tyrosinase inhibition evaluation

The inhibitory activity of compounds 1–14 were evaluated on the diphenolase activity of mushroom tyrosinase using L-dopa as the substrate and Kojic acid as a standard. The inhibitory activity of compounds 1-14was screened at the concentrations of 0.2 mM, 0.4 mM, 0.6 mM, 0.8 mM and 1 mM, respectively. The inhibition percentage and IC_{50} values were calculated and the inhibition curves have been obtained by Graphpad Prism 8.0 software. The experimental results and the structures of compounds 1–14 were listed in Table 1. Firstly, all target compounds, except for compounds 2, 3, 7 and 9, exhibited inhibitory activity on mushroom tyrosinase with the inhibitory rates of over 60% at the concentration of 1 mM, and the inhibition rates of compounds 8, 13, and 14 were 78.8%, 82.4% and 80.6%, respectively.

In addition, the concentration-effect curve of compounds 8, 13 and 14 were tested at 10 different concentrations, the inhibition curves were showed in Fig. 2. In order to comparetothe parent compound, the

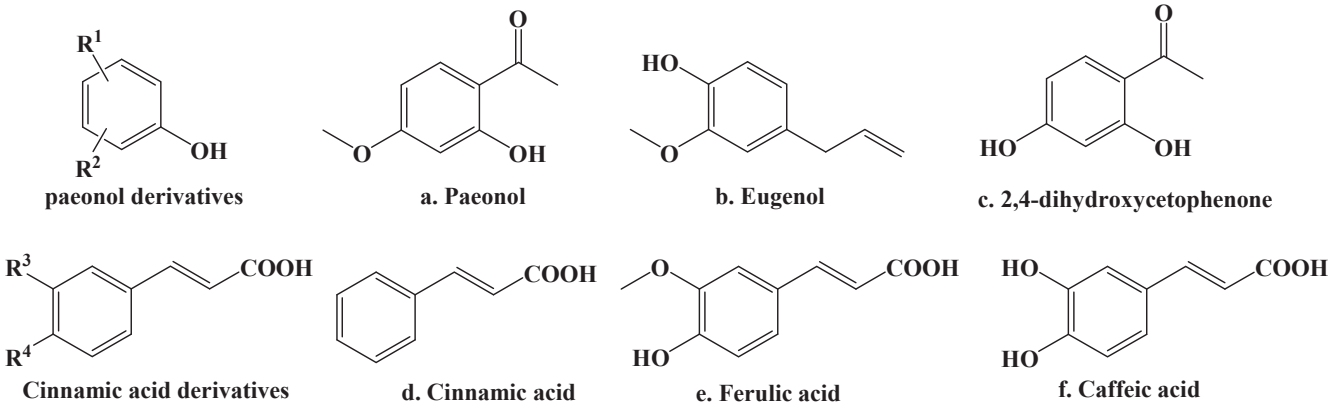

Fig. 1. The structures of lead compounds: the paeonol and cinnamic derivatives.

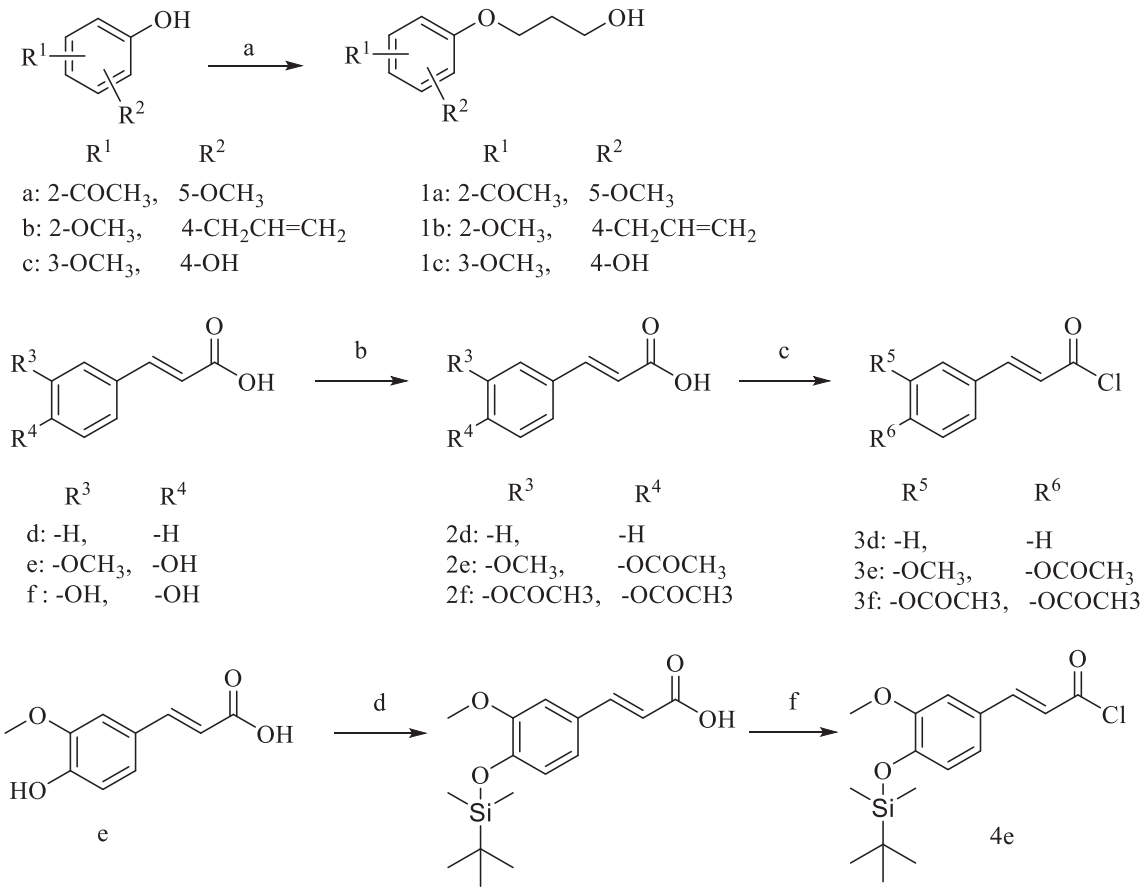

R^1	R^2
a: 2-$COCH_3$,	5-OCH_3
b: 2-OCH_3,	4-$CH_2CH{=}CH_2$
c: 3-OCH_3,	4-OH

R^1	R^2
1a: 2-$COCH_3$,	5-OCH_3
1b: 2-OCH_3,	4-$CH_2CH{=}CH_2$
1c: 3-OCH_3,	4-OH

R^3	R^4
d: -H,	-H
e: -OCH_3,	-OH
f : -OH,	-OH

R^3	R^4
2d: -H,	-H
2e: -OCH_3,	-$OCOCH_3$
2f: -OCOCH3,	-OCOCH3

R^5	R^6
3d: -H,	-H
3e: -OCH_3,	-$OCOCH_3$
3f: -OCOCH3,	-OCOCH3

Scheme 1. Synthesis routes of intermediate compounds 1a-1c, 3d-3f and 4e. Reagents and conditions: (a) acetone, K_2CO_3, BrC_3H_6OH, reflux, 6 h; (b) $(CH_3CO)_2O$, 4 h, reflux; (c) $SOCl_2$, DCM, reflux, 5 h; (d) TBDMSCl, Et_3N, DCM, 0 °C to rt, 4 h; (e) $SOCl_2$, DCM, reflux, 5 h.

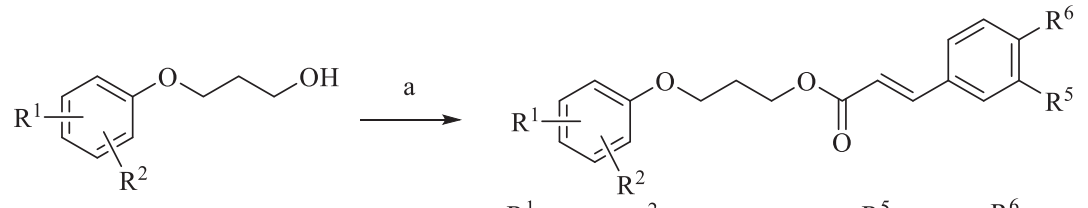

R^1	R^2
1a: 2-$COCH_3$,	5-OCH_3
1b: 2-OCH_3,	4-$CH_2CH{=}CH_2$
1c: 4-$COCH_3$,	3-OH

	R^1	R^2	R^5	R^6
1:	2-$COCH_3$	5-OCH_3	-OCH_3	-$OCOCH_3$
2:	2-$COCH_3$	5-OCH_3	-$OCOCH_3$	-$OCOCH_3$
3:	2-$COCH_3$	5-OCH_3	-H	-H
4:	4-$COCH_3$,	3-OH	-OCH_3	-$OCOCH_3$
5:	4-$COCH_3$,	3-OH	-$OCOCH_3$	-$OCOCH_3$
6:	2-OCH_3,	4-$CH_2CH{=}CH_2$	-$OCOCH_3$	-$OCOCH_3$
7:	2-OCH_3,	4-$CH_2CH{=}CH_2$	-OCH_3	-$OCOCH_3$
8:	4-$COCH_3$,	3-OH	-H	-H
9:	2-OCH_3,	4-$CH_2CH{=}CH_2$	-H	-H
10:	2-$COCH_3$	5-OCH_3	-OCH_3	-$Si(CH_3)_2C(CH_3)_3$
11:	4-$COCH_3$,	3-OH	-OCH_3	-$Si(CH_3)_2C(CH_3)_3$
12:	2-OCH_3,	4-$CH_2CH{=}CH_2$	-OCH_3	-$Si(CH_3)_2C(CH_3)_3$

Scheme 2. Synthesis routes of intermediate compounds 1a-1c, 3d-3f and 4e. Reagents and conditions: (a) Pyridine, DCM(dried by $MgSO_4$), −10 °C or rt, overnight.

inhibitory activity was evaluated at the same concentration. The results showed that the IC_{50} values of the parent compounds were from 154.6 μM to 1135.8 μM, the IC_{50} values of the 14 compounds were lower than the parent compound except for compound 2, 3, 7 and 9, which suggested that the inhibitory activity of these compounds were significantly improved. Especially, the IC_{50} values of compounds 8, 13 and 14 were 20.7 μM, 13.9 μM and 15.1 μM, respectively. Among these target compounds, 1–9 and 10–14 were two series of cinnamic acid ester

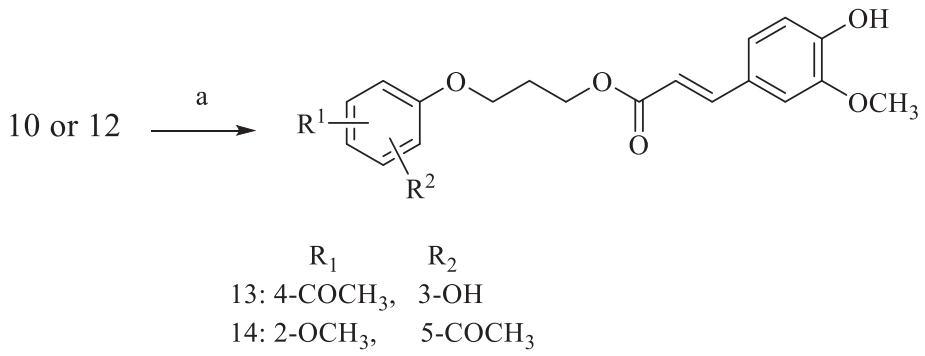

Scheme 3. The synthetic route of novel tyrosinase inhibitors 13–14 based on natural product scaffolds. Reagents and conditions: (a) Tetrabulammonium fluoride, rt, 2 h.

Table 1
The inhibition percentage of target compounds 1–14 on enzymatic-based tyrosinase activity at the concentration of 1 mM.

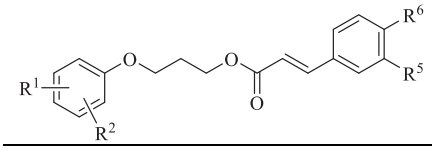

Compound	R^1	R^2	R^5	R^6	Inhibition (%)	IC_{50}
1	2-$COCH_3$	5-OCH_3	OCH_3	$OCOCH_3$	75.8 ± 1.73	130.5 ± 5.55
2	2-$COCH_3$	5-OCH_3	$OCOCH_3$	$OCOCH_3$	54.6 ± 0.88	411.8 ± 29.5
3	2-$COCH_3$	5-OCH_3	H	H	49.2 ± 2.96	226.1 ± 20.86
4	4-$COCH_3$	3-OH	OCH_3	$OCOCH_3$	75.1 ± 2.81	85.72 ± 18.53
5	4-$COCH_3$	3-OH	$OCOCH_3$	$OCOCH_3$	70.6 ± 2.41	138.6 ± 16.33
6	2-OCH_3	4-$CH_2CH=CH_2$	$OCOCH_3$	$OCOCH_3$	75.3 ± 1.59	83.4–169
7	2-OCH_3	4-$CH_2CH=CH_2$	OCH_3	$OCOCH_3$	58.4 ± 1.61	214.6 ± 4.77
8	4-$COCH_3$	3-OH	H	H	78.8 ± 2.42	20.7 ± 3.51
9	2-OCH_3	4-$CH_2CH=CH_2$	H	H	59.5 ± 2.86	411.8 ± 21.01
10	2-$COCH_3$	5-OCH_3	OCH_3	TBDMS-	65.2 ± 2.59	120.2 ± 18.53
11	4-COCH3	3-OH	OCH_3	TBDMS-	69.8 ± 2.71	25.37 ± 7.56
12	2-OCH_3	4-$CH_2CH=CH_2$	OCH_3	TBDMS-	59.6 ± 1.56	126.7 ± 11.7
13	4-$COCH_3$	3-OH	OCH_3	OH	82.4 ± 1.36	13.98 ± 5.44
14	2-OCH_3	5-$COCH_3$	OCH_3	OH	80.6 ± 1.70	15.16 ± 4.763
Ferulic					71.1 ± 2.57	154.6 ± 20.44
Caffeic acid					68.8 ± 2.42	169.2 ± 16.87
Cinnamic					45.7 ± 2.25	>1000
Peaonol					70.2 ± 1.17	336.1 ± 17.02
Eugenol					56.4 ± 1.47	566.4 ± 28.25
2,4-Dihydroxyacetophenone					45.1 ± 2.46	>1000
kojic					81.8 ± 1.84	30.83 ± 7.56

Notes: Values represent the mean ± standard deviation (SD) of mushroom tyrosinase inhibition experiments (n = 3); In the result of IC_{50} values, the concentration of these compounds were 0.2, 0.4, 0.6, 0.8 and 1.0 mM respectively (n = 3).

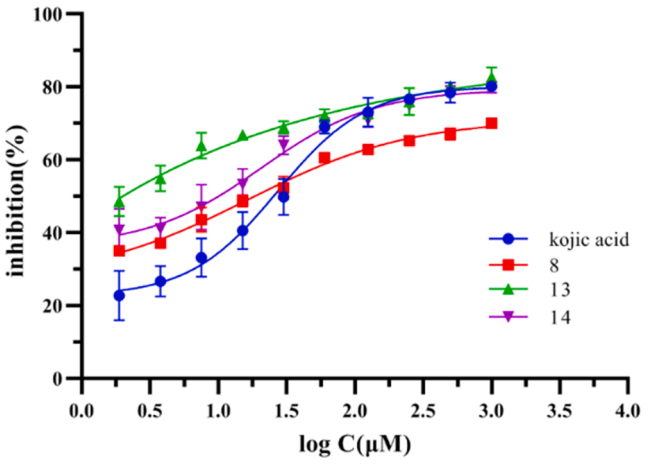

Fig. 2. The concentration-inhibition curve of tyrosinase inhibition of 8, 13, 14 and kojic acid.

compounds, and the difference among themwasthe number of phenolic hydroxyl groups. With the increasing of the phenolic hydroxyl group number, the IC_{50} values were decreasing and inhibitory rates were improved. The higher the number of phenolic hydroxyl groups, the smaller the IC_{50} and the stronger the inhibitory activity. The activity decreased significantly when the corresponding phenolic hydroxyl group was replaced.

The study on structure–activity relationship indicated that the phenolic hydroxyl group may be the important active group for the inhibition of tyrosinase activity, which was closely connected with the number of phenolic hydroxyl groups and result shows: di-phenols > mono-phenols > non-phenol compounds. The inhibitory activity of compounds 13 and 14 was 2.3 and 2 times than the positive drug kojic acid respectively.

2.3. The inhibition mechanism study

The inhibition mechanism of compound 8, 13 and 14 were investigated based on the results of inhibition type and kinetic study, the method is similar with 4.2.2, but the concentration of L-dopa and

mushroom tyrosinase with slight modification. The relationship between enzyme activity and its concentration in the presence of compound 8, 13 and 14 plots of the remaining enzyme activity versus the enzyme concentration at the different inhibitor concentrations given a set of straight line, which all pass through the origin (Fig. 3. 8-a, 13-a and 14-a). Increasing the inhibitors concentration reduced the slope of the line, indicating that the inhibitor reduced the activity of the enzyme. Thus, the diphenolase activity of compounds 8, 13 and 14 on tyrosinase was reversible type inhibition.

The kinetic data of compound 8, 13 and 14 on the L-dopa oxidation were expressed by Lineweaver-Burk double-reciprocal plots. For compound 13, the plots of *1/v* versus *1/[S]*to give a group of straight lines with different slopes that intersect the vary point on the X-axis (Fig. 3. 13-b), suggesting that the K_m remains the same, while V_{max} decreases with increasing concentrations of compound 13. The results indicated that the inhibition type of compound 13 was non-competitive with a K_i value of 12.3 μM, which means that the binding site of 13 with tyrosinase is not the active site. This result also reflects that the compound 13 reduces the activity of tyrosinase whether or not it is already bound to the substrate. A series of straight lines intercept at the point in the second quadrant that compounds 8 and 14 were mixed type inhibitors with a K_i value of 88.49 μM and 12.30 μM, and K_{is} value of 238.09 μM and 17.54 μM, respectively (Fig. 3, Table 2 and Fig. 4). Meanwhile, this result suggested that compounds 8 and 14 were both mixed-type inhibitors and indicated that they bind not only with the free enzyme but also with the enzyme-substrate complex. This complex could prevent the free oxygen molecule taking part in the oxidation of o-diphenols and cause tyrosinase to lose catalytic ability. The inner mechanism of inhibitor had been discussed through the results of molecular docking.

2.4. Cytotoxicity of compounds 8, 13 and 14 in B16F10 cells

The cell viability of compounds 8, 13 and 14 was measured and evaluated using the $B_{16}F_{10}$ cell line. These compounds acted on the cells at concentrations of 25, 50, 100, and 200 μM for 24 h. The arbutin and kojic acid were used in positive groups and the experimental results were showed in Fig. 5. Compound 8 with the values of 79.13% showed that a certain cytotoxicity compared with compounds 13 and 14 with the values of 85.96% and 88.47% at the average level of 200 μM. Compounds 13 and 14 were safer than kojic acid and arbutin at the concentration in the range of 100 μM and the values were 91.99% and 91.96%, respectively. Furthermore, single-factor analysis showed that compounds 13 and 14 were not significant difference with the control group in the cell survival rate at the concentration lower than 100 μM ($P < 0.05$), indicating compounds 13 and 14 have high safety.

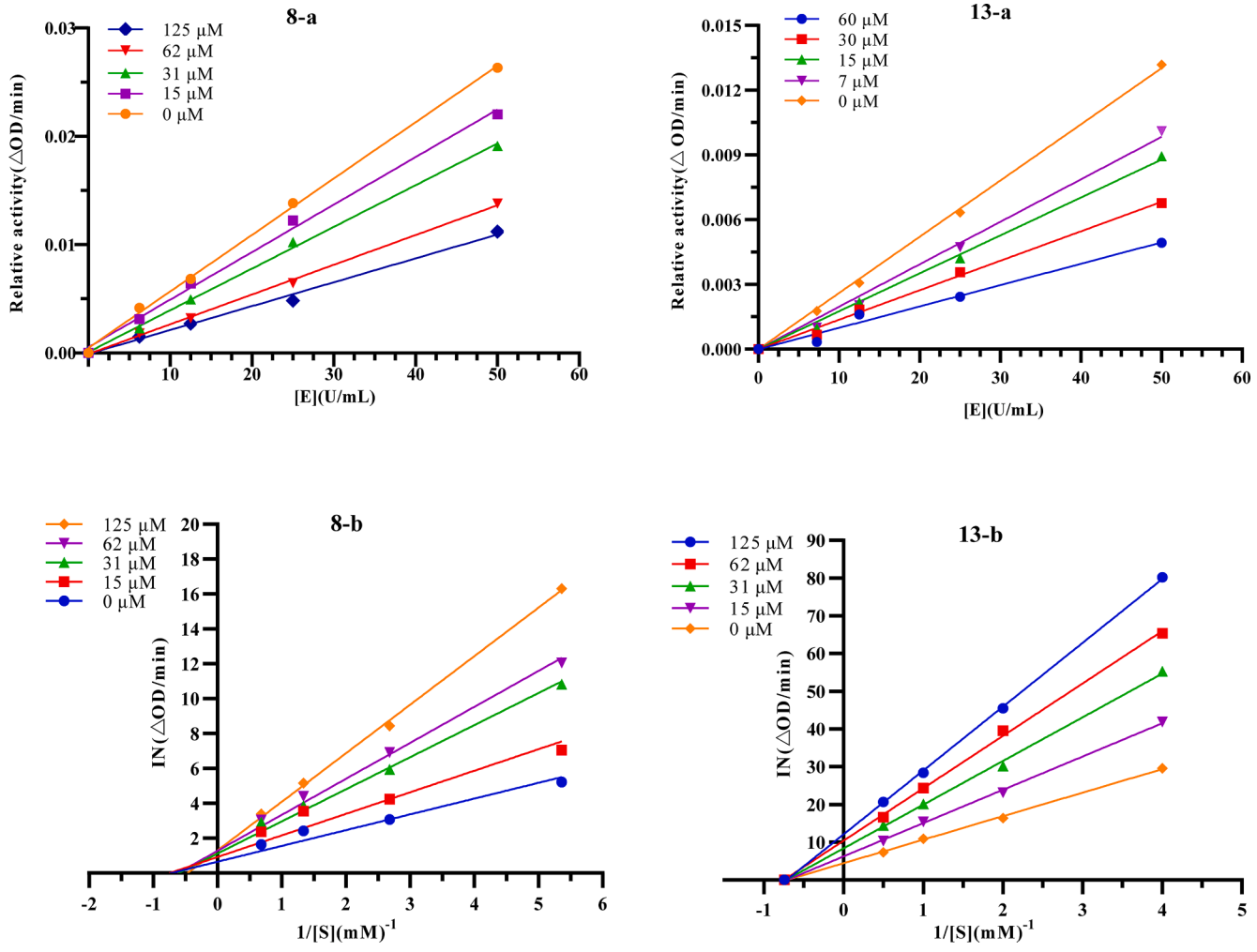

Fig. 3. Determination of the inhibition mechanism on diphenolase activity mushroom tyrosinase by compound 8, 13 and 14: The Fig. 8-a, 13-a and 14-a represent effects of tyrosinase concentrations on its diphenolase activity at different concentrations of inhibitors. The concentrations of compound 8 for curves were 0, 15, 31, 62 and 125 μM, compound 13 and 14 for curves were 0, 7, 15, 31 and 62 μM espectively; Lineweaver-Burk plots (8-b, 13-b and 14-b) for mushroom tyrosinase with L-dopa as substrate in the presence of compound 8, 13 and 14. The concentrations of compound 8 and 13 for curves were 0, 15, 31, 62 and 125 μM, compound 14 for curves were 0, 7, 15, 31 and 62 μM espectively.

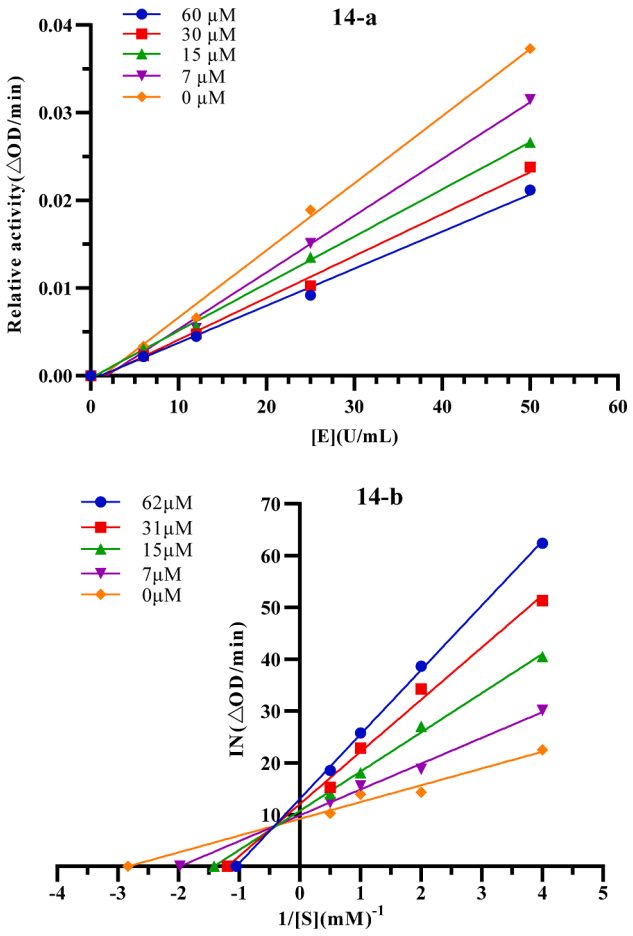

Fig. 3. (*continued*).

Table 2
The inhibition mechanism, K_i and K_{is} values of compounds 8, 13 and 14.

Compounds	Inhibition type	K_i (μM)	K_{is} (μM)
8	Mixed type	88.49	238.09
13	Non-competitive	6.81	17.18
14	Mixed type	12.3	17.54

2.5. The anti-melanogenesis activity of compounds 8, 13 and 14 in B16F10 cells

In the model group, 1 μM α-MSH (melanin-promoting hormone) was added to enhance the melanin content and stabilize the melanin content in melanocytes. Kojic acid and arbutin were used as positive control. Results of anti-melanogenesis inhibition experiments showed that the three compounds 8, 13 and 14 were significantly different with the model group at 200 μM and showed a certain degree of concentration dependence. The α-MSH model group showed extremely significant statistical differences with the control group. Compounds 8, 13 and 14 suppressed the melanin production with the inhibition ratio values of 19.62%, 23.83%, and 20.59%, respectively. Among which compound 13 had the highest anti-melanogenic activity (Fig. 6).

2.6. Cell tyrosinase inhibitory activity:

The inhibitory effects of compounds 8, 13 and 14 on the tyrosinase activity of B16F10 cells were showed in Fig. 7. The control group was normal B16F10 cells, and the experiment results showed that three compounds had significant differences compared with the control group at the 200 μM and 100 μM ($P < 0.05$). The compound 14 showed a moderate inhibitory activity at 100 μM, but compound 8 and 13 showed strong tyrosinase inhibitory activity with inhibition rate of 20.59% and 23.83%, respectively. Especially compound 13 have the highest inhibitory activity, which was higher than that of kojic acid and arbutin (19.21% and 20.45%) at the same concentration level, and have a certain degree of concentration dependence. In addition, the cytotoxicity of compound 8 at 100 μM was higher than that of compounds 13 and 14, indicating that the tyrosinase inhibitory activity has no direct relationship with cytotoxicity, it also proved that compounds 13 and 14 were indeed stronger and safe cell tyrosinase inhibitor.

In summary, the comprehensive results of the mushroom tyrosinase activity inhibition experiment and relevant cell experiments showed that compound 13 has a higher inhibitory activity on B16F10 cells tyrosinase, and the cytotoxicity was lower than compounds 8 and 14. In addition, compounds 13 and 14 have lower cytotoxicity than kojic acid and compounds 8 at 100 μM. Among the cell tyrosinase inhibitory activity, compound 13 exhibited the strongest inhibitory activity at the concentration of 50 μM and 100 μM. In the conclusion, compound 13 displayed better activity than other inhibitors in cellular tyrosinase inhibitory activity experiment.

2.7. Antioxidant activity

Tyrosinase catalyzes biosynthesis of melanin involved in oxidation of o-diphenols to the corresponding o-quinones [6]. Therefore, the antioxidant activities of compound 8, 13, 14 were measured with Vc as a positive control and the results were presented in Fig. 8 in the form of DPPH radical scavenging activity. The half maximal effective concentrations (EC_{50}) of compound 13 and V_c were calculated by Graph Pad

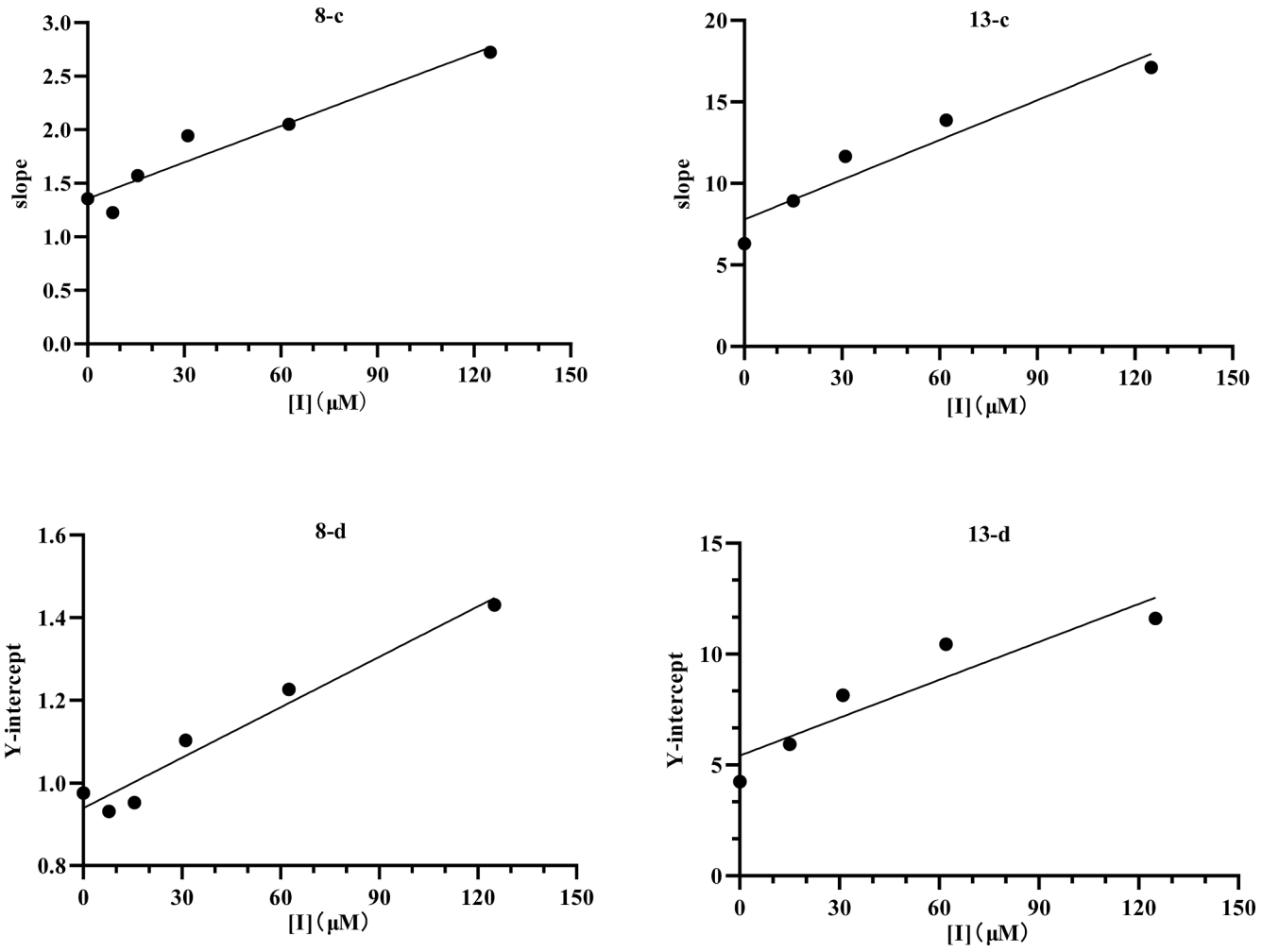

Fig. 4. The determination of the inhibition constant K_i and K_{is}: The Fig. 8-c, 13-c and 14-c represent the plot of slope versus the concentration of 8, 13 and 14 for the determination of the inhibition constant K_i respectively. The Fig. 8-d, 13-d and 14-d represent the plot of intercept versus the concentration of 8, 12 and 13 for the determination of the inhibition constant K_{is} respectively.

Prism 8.0.2, and also were listed in Fig. 8. As shown in Fig. 8, obviously, the DPPH radical scavenging activity of compound 13 was higher than those of compound 8 and 14 with EC50 of 0.14 mmol/L. The EC50 of compound 8 and 14 were not determined under 4 mmol/L due to their poor DPPH radical scavenging activity. Compound 13 has two phenolic hydroxyl groups, compound 8 and 14 just have one hydroxyl group, perhaps the introduction of the second hydroxyl group resulted in the increase in DPPH radical scavenging activity of Compound 13. Vc has been widely applied as an antioxidant and a positive control in antioxidant experiment because of its excellent antioxidant activities. In this study, the EC_{50} of Vc and compound 13 were 0.03, 0.14 mmol/L, respectively, which showed that compound 13 was a potential antioxidant.

2.8. Molecular docking analyses

As compounds 8, 13 and 14 exhibited better mushroom tyrosinase inhibition than the other cinnamyl-paeonol derivatives, Cellular tyrosinase inhibitory activity molecular docking was introduced to predict the docking conformation of these three compounds(Fig. 9 group A and group B). The construction of molecular and the analyses of docking were possessed as delineated between 2Y9X and the active compounds 8, 13, 14, kojic acid and arbutin in the subsequent section. Kojic acid and arbutin were used reference to using the same active site and method. The active site 5 (-29.76; −10.28; −42.21) was screened out and 12.0000 was selected as the radius of activity site. It is repositioned in the cavity of the enzyme protein to obtain the ligand molecule and the enzyme amino acid residue. Finally, two-dimensional diagram of the interaction was showed in Fig. 9, group B. The lowest energy conformation of the enzyme inhibitor complex has been calculated and predicted through intermolecular hydrogen bond donors and interactions. The binding affinity of the enzyme inhibitor complex during the docking process was calculated, not only taking into consideration the best score indicating the matching energy, but also including the best conformation to achieve geometric matching and eliminating adverse interactions. Small molecule inhibitors and tyrosine results of acid enzyme affinity scores showed in Table 3.

Furthermore, the type of functional groups determined the interactions in the enzyme-inhibitor complexes. The results of docking were also basically kept up with the rule of structure–activity relationship. The phenolic hydroxyl group in cinnamyl derivatives contributes to the binding affinity of the enzyme-inhibitor complexes. It was not doubted that the number of phenolic hydroxyl groups and ester bonds played essential roles in interacting protein. The result of docking score showed that compound 8, 13 and 14 performed better than the original ligand as kojic acid and arbutin. Among of those compounds, the compound 13 exerted the best interaction with the protein, which was partly different with the result of the enzyme inhibition test. Generally, a

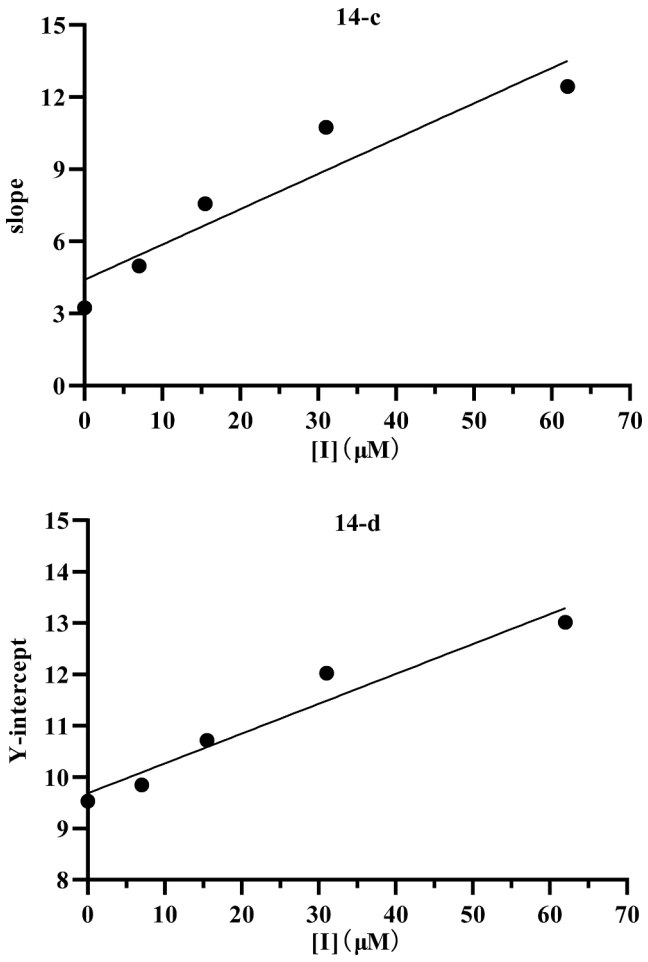

Fig. 4. (*continued*).

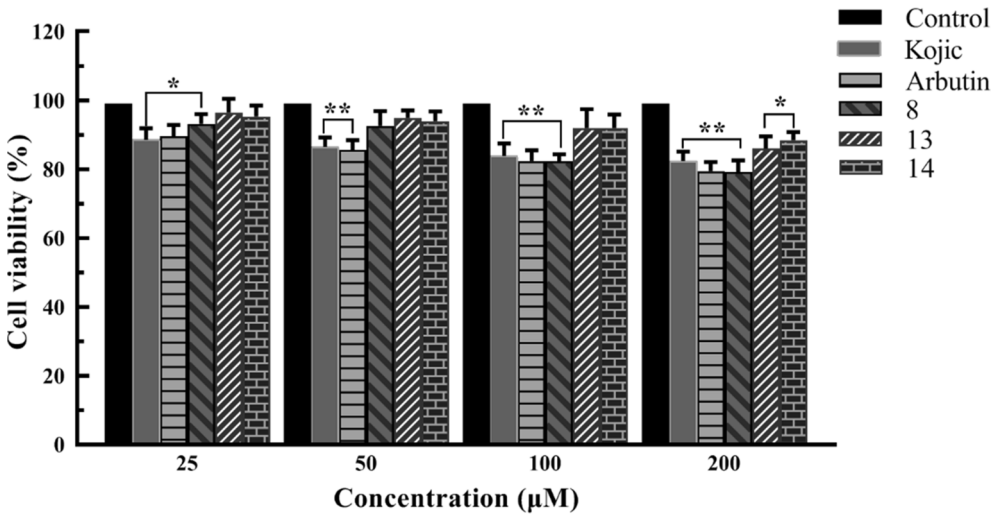

Fig. 5. Cytotoxicity of compounds 8, 13 and 14; Notes: n = 3,*$P < 0.05$,**: $P < 0.01$, (with control group).

hydrogen bond was found between kojic acid and Arbutin with Gln74, Tyr98 and Tyr78 (Fig. 9-B Compound kojic acid and arbutin). Other interactions were also discovered including Van der Waals force between inhibitor with Leu 77, His76, Thr324 (Fig. 9-B Compound kojic acid). On the one hand, this result revealed that compound 13 has not interacted with copper ions through polar contacts, but it has interaction with Gln48, Asp10, Glv68 through affection of Hydrogen bonds, the interactions of Pi-Anlon with Asp10 was also formed (Fig. 9-B Compound 14).

On the other hand, hydrogen bonds was found, which came from the ester group with Lys70 to compound 8 between protein and ligand, and ester group interacts with Lys5 and Met325 through electrostatic attraction benzene ring (Fig. 9-B Comopund 8). Moreover, the compound 13 showed potential interaction with the active site, which

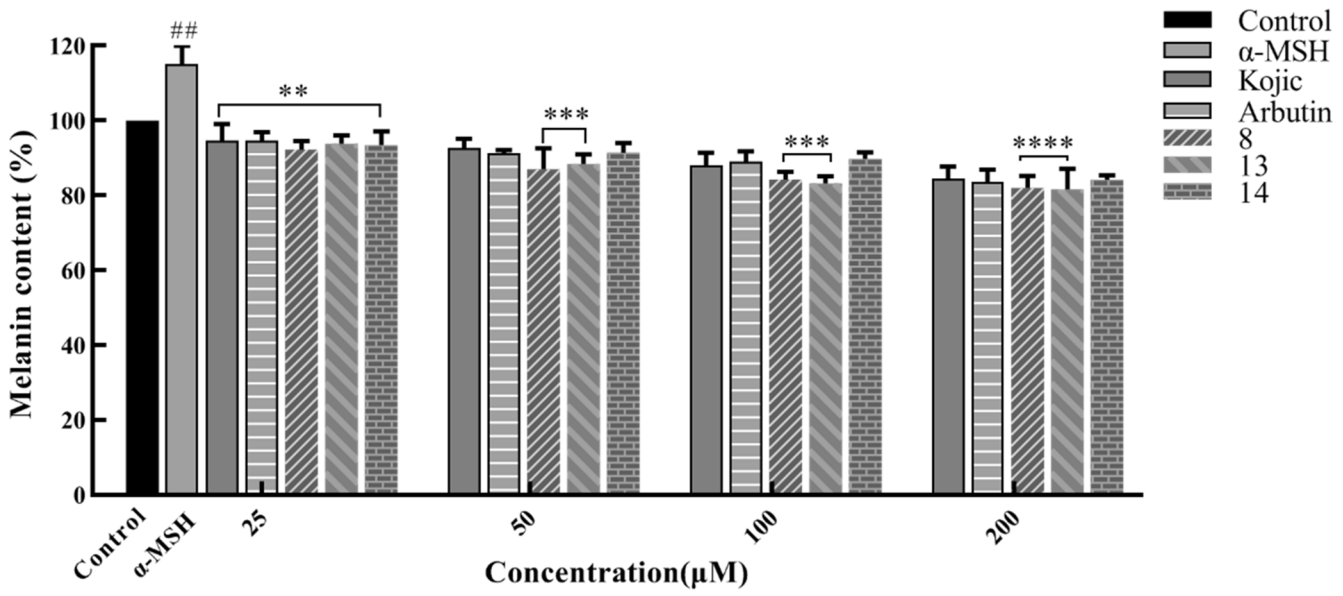

Fig. 6. Melanin production inhibitory effect of compounds 8, 11, 13 and 14 in B16F10 melanoma cells. Notes: n = 3, $^{\#\#}$: $P < 0.01$(compared with control group), **: $P < 0.01$, ***: $P < 0.001$, ****: $P < 0.0001$ (compared with model group);

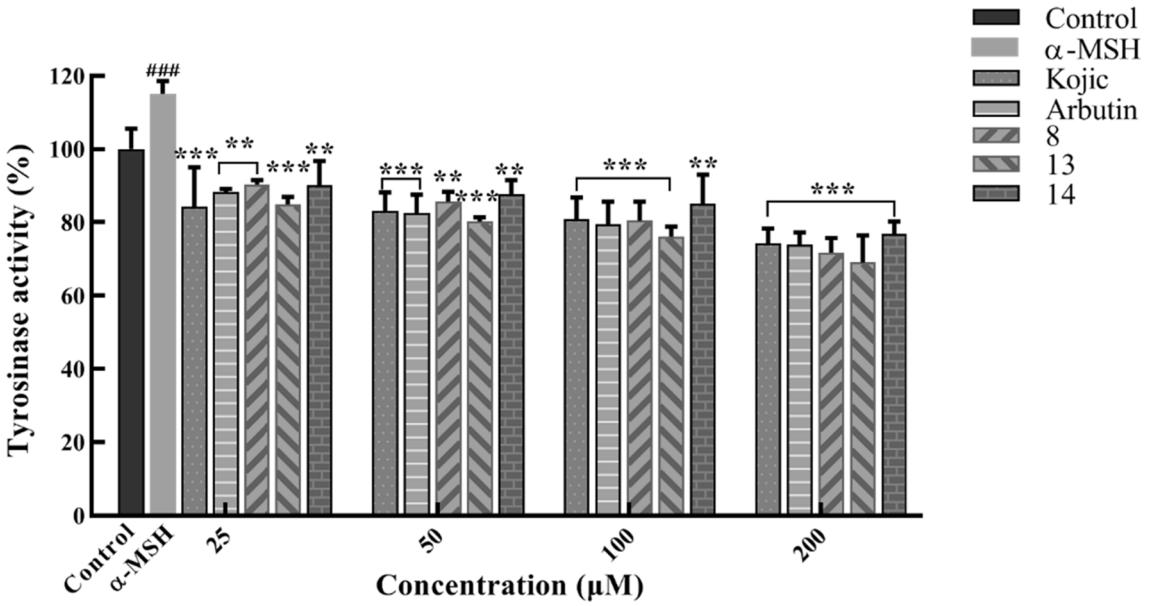

Fig. 7. Cellular tyrosinase inhibitory activity of compounds 8, 13 and 14 in B_{16} F_{10} melanoma cells. Notes: n = 3, *: $P < 0.05$, **: $P < 0.01$, ***: $P < 0.001$(compared with model group).

provided evidence for the result of stronger inhibition activity of tyrosinase. On the basis of molecular docking, the result indicated that the basic moiety of arginine showed electron donating property. The covalent H has easily to form H-bond with electrophilic O atom in the ester group and phenolic hydroxyl group. The docking result revealed that the phenolic hydroxyl could enhance the binding affinity of the enzyme-inhibitor complexes. Compared with compounds 8 and 14, both just with one phenolic hydroxyl, compound 13 has two phenolic hydroxyls and exhibited the best tyrosinase inhibition activity among these three compounds.

The kinetics study showed that compound 13 was a non-competitive inhibitor, while compounds 8 and 14 were a mixed-type inhibitor. The docking studies of the compound 14 contribute to explain the difference to a degree. The results also revealed that the functional group of the cinnamic-phenol ester derivatives mostly depends on the phenolic hydroxyl moiety. The hydroxyl group of compound 13 did not insert into the active site of tyrosinase, which was in agreement with the results of the kinetics study.

3. Conclusions

Fourteen cinnamic ester derivatives have been designed and synthesized as tyrosinase inhibitors by ester reaction. The result of mushroom tyrosinase test exhibited that compounds 8, 13 and 14 have better inhibition at 1 mM than kojic acid and the lower IC_{50} values. Especially, compound 13 with IC_{50} value of 13.9 μM showed tyrosinase inhibitory activity 2.2 times better than that of kojic acid with IC_{50} value of 30.83 μM. In addition, inhibition on tyrosinase and melanin content indicated that compound 13 displayed better activity than other inhibitors in the B16F10 melanoma cells, which the cell viability was higher than

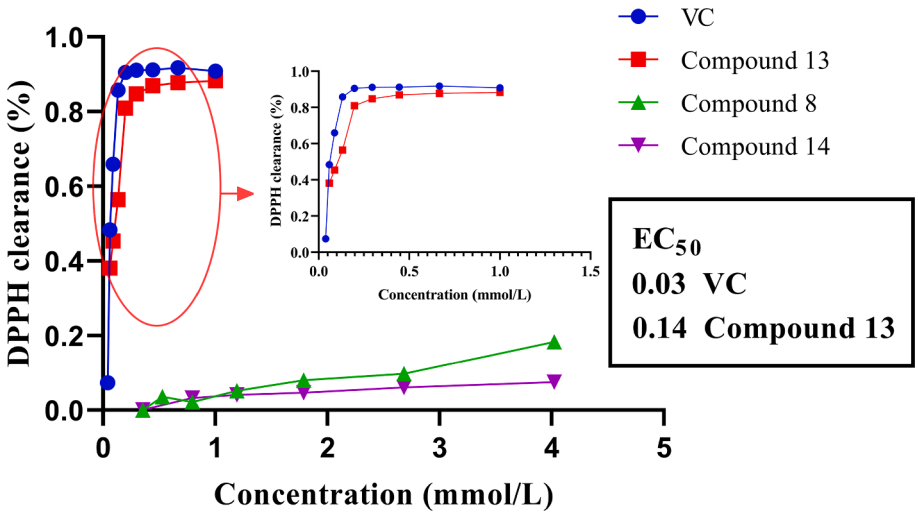

Fig. 8. DPPH radical scavenging capacities of compounds 8, 13, 14, Vc and the EC_{50} of Vc and compound 13.

compound 8 and kojic acid at 100 μM. In the cell tyrosinase inhibitory activity, compound 13 exhibited the strongest inhibitory activity at the concentration of 50 and 100 μM. Furthermore, kinetic mechanism suggested that the competitive mode of compound 13 was non-competitive manner. In the antioxidant experiment, compound 13 exhibited a certain extent antioxidant ability. Molecular docking analysis performed that the main type of interactive bind with active site was Hydrogen bond. Summarizing these results, compound 13 was proved to be most potential tyrosinase inhibitor and anti-melanogenesis agents in these 14 derivatives.

4. Experimental section

4.1. Chemistry

4.1.1. General procedures for synthesis of compounds 1a-c:

*4.1.1.1. 1-(2-(3-hydroxypropoxy)-4-methoxyphenyl)ethan-1-ketone (compound **1a**).* 3-Bromo-1-propanol (2.0 mM, 2 eq) was added to a solution of compound a (1.0 mM, 1 eq) in acetone solution, and then added extra dry K_2CO_3 (0.6 mM, 0.6 eq), the mixture was stirred under reflux at 76 °C for 6 h. The reaction was monitored by TLC, the mixture was concentrated under reduced pressure after reaction finished. Then the residue was dissolved in Ethyl acetate, washed with brine. The slight yellow organic layer was dried with $MgSO_4$, and then concentrated under reduced pressure to give a bright yellow oil as an intermediate, which was purified by flash chromatography to gain 1a as a light yellow oil (Yield: 60%).

*4.1.1.2. 1-(2-hydroxy-5-(3-hydroxypropoxy)phenyl)ethan-1-ketone (compunds**1b**).* The synthesis method was similar with compound 1a, which was a white crystal (Yield: 85%).

*4.1.1.3. 3-(4-allyl-2-methoxyphenoxy)propan-1-ol (compunds**1c**).* The synthesis method was similar with compound 1a, which was a light oil (Yield: 72%).

4.1.2. General procedures for synthesis of compounds **3d-f:**

*4.1.2.1. Cinnamoyl chloride (compounds **3d**).* Excess acetic anhydride was added to compound d (5 mM, 1 eq), and the mixture was refluxed for 5 h at 140 °C. The mixture was concentrated under reduced pressure after reaction finished to gain immediate. $SOCl_2$ (5 mL, 15 mM) was added to a solution of the immediate (3.0 mM) in DCM (20 mL), and the mixture was refluxed for 5 h at 75 °C. Then the solution was heated to 85 °C for evaporation. After cooling to room temperature, and then concentrated under reduced pressure to obtain yellow solution 3d (yield: 75–85%);

*4.1.2.2. (E)-4-(3-chloro-3-oxoprop-1-en-1-yl)-2-methoxyphenyl acetate (compunds **3e**).* Compound e replaced compounds d as material, others synthesis procedures was similar with compound 3d, which was yellow solid.

Compound e replaced compounds d as material, others synthesis procedures was similar with compound 3d, which was a yellow solid.

*4.1.2.3. (E)-4-(3-chloro-3-oxoprop-1-en-1-yl)-1,2-phenylene diacetate (Compound **3f**).* Compound f replaced compounds d as material, others procedures as the same as compound 3d, which was a yellow solid.

4.1.3. (E)-3-(4-((tert-butyldimethylsilyl)oxy)-3-methoxyphenyl)acryloyl chloride (compounds **4e**)

Tert-butyldimethylsilyl chloride (6 mM, 2 eq) was added to a suspension of compounds e (3 mM, 1 eq) in 100 mL DCM at 0 °C, and then NEt_3 (3 mM, 1 eq)was added slowly. The mixture was stirred at room temperature for 4 h after 1 h. The mixture was washed with water and brine respectively. The organic layer was dried with $MgSO_4$, and then concentrated under reduced pressure to give a bright yellow oil as an intermediate, which was purified by flash chromatography to get 4e as a white power (Yield: 91.6%).

*4.1.3.1. (E)-3-(2-acetyl-5-methoxyphenoxy) propyl 3-(3-methoxy-4-(prop-1-en-2-yloxy) phenyl) acrylate (compound **1**).* The residue 1a (0.7 mM, 1 eq) was dissolved in dry DCM, added 2d (1 mM, 1.3 eq) at 0 °C, and then added NEt_3 (0.7 mM, 1 eq), which was stirred at room temperature overnight, the reaction system was monitored by TLC. The mixture was washed with 1 M HCl solution, saturated $NaHCO_3$ and brine respectively. The organic layer was dried with $MgSO_4$, and concentrated to give a crude product, which was purified by chromatography on silica gel using petroleum ether/ethyl acetate (2:1, v:v) as original eluent to get the etherification product 1.

White crystal. m.p. 110–111 °C. Yield: 56%; ^{1}H NMR (400 MHz, $CDCl_3$) δ: 7.85 (d, J = 8.7 Hz, 1H), 7.66 (t, J = 10.9 Hz, 1H), 7.12 (d, J = 8.0 Hz, 1H), 7.05 (d, J = 8.0 Hz, 1H), 6.53 (d, J = 8.7, 1H), 6.46 (d, J = 10.9 Hz, 1H), 6.38 (d, J = 15.9 Hz, 1H), 4.44 (t, J = 6.2 Hz, 2H), 4.18 (t, J = 6.1 Hz, 2H), 3.86 (t, J = 6.7 Hz, 6H), 2.61 (s, 3H), 2.32 (s, 3H), 2.19–2.16(m, 2H); ^{13}C NMR (100 MHz, $CDCl_3$) δ: 197.71, 168.97, 166.82, 164.54, 160.22, 151.45, 141.53, 132.91, 117.94, 111.26,

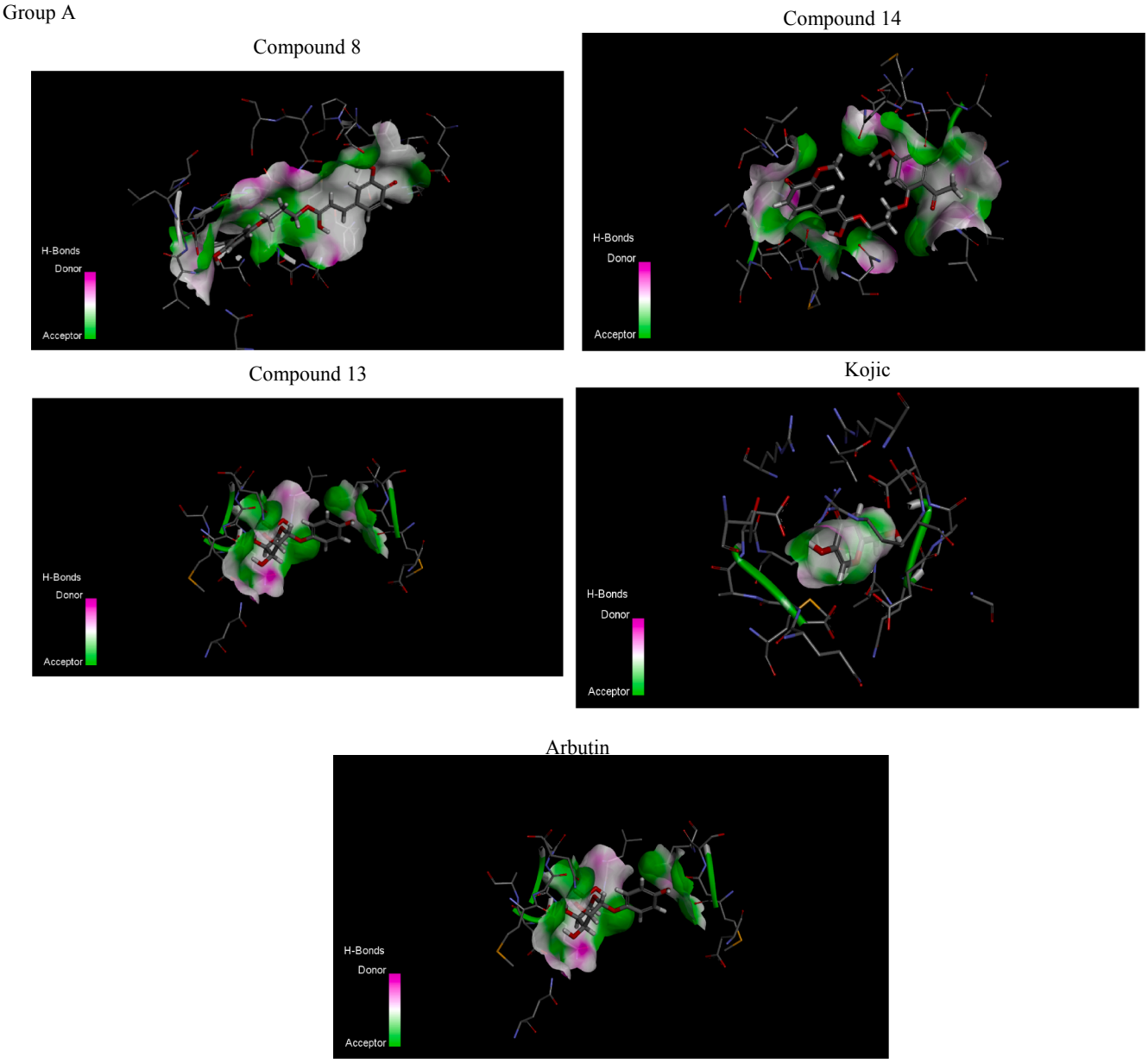

Fig. 9. Ligand-protein interaction of compounds 8, 13, 14, kojic acid and arbutin with the active site of mushroom tyrosinase (2Y9X) has been fulfilled by Discovery Studio 2019. These two groups pictures displayed interaction of compound 8, 13, 14, kojic acid and arbutin with the enzyme, respectively. The pictures in group A show the 3D docking of ligands in the active binding pocket with the hydrophobic effect area displayed; The pictures in group B showed the 2D interaction pattern between the ligands and animo acid residue, the bottom of these figures in group B represents the important interactions type between the ligand atoms and the amino acid residues of the protein.

105.18, 99.06, 65.14, 61.43, 55.99, 55.66, 32.27, 28.78, 20.78; IR (cm^{-1}) 2976.23, 2331.06, 1720.48, 1605.26, 1580.56, 1551.26, 1414.64, 1279.38, 1246.35, 1225.36, 1030.18, 1002.64, 750.42, 716.24. HRMS (ESI, positive) *m/z* calcd for $C_{24}H_{26}O_8$ $[M]^+$:442.4640, found: 441.3437.

*4.1.3.2. (E)-4-(3-(3-(2-acetyl-5-methoxyphenoxy) propoxy)-3-oxoprop-1-en-1-yl)-1, 2-phenylene diacetate(compound **2**).*. Compound 2e replaced compounds 2d as material, others procedures as the same as compound 1.

White crystal. m.p. 126–127 °C. Yield: 71%; ^{1}H NMR (400 MHz, $CDCl_3$) δ7.86 (d, J = 1.0 Hz, 1H), 7.83 (d, J = 1.0 Hz, 1H), 7.65 (s, 1H), 7.61 (s, 1H), 7.41 (s, 1H), 7.39 (s, 1H), 7.36 (s, 1H), 7.26 (s, 1H), 7.23 (s, 1H), 7.21 (s, 1H), 6.53 (d, J = 10.0 Hz, 2H), 6.45 (s, 2H), 6.40 (s, 1H), 6.36 (s, 1H), 4.43 (t, J = 6.2 Hz, 3H), 4.17 (t, J = 6.1 Hz, 3H), 3.84 (d, J = 1.0 Hz, 3H), 2.61 (d, J = 1.0 Hz, 3H), 2.30 (d, J = 2.4 Hz, 3H), 2.27 (m, J = 6.1 Hz, 2H), 2.17 (s, 2H); ^{13}C NMR (100 MHz, $CDCl_3$) δ197.93, 177.73, 166.58, 164.56, 160.23, 143.35, 142.50, 132.92, 124.10, 122.87, 118.93, 105.26, 99.02, 65.09, 61.48, 55.67, 32.27, 28.73, 20.76; IR(cm^{-1})2955.64, 1780.24, 1750.35, 1630.24, 1580.64, 1496.51, 1410.38, 1382.36, 1366.35, 1010.94, 820.64, 704.52, 650.32. HRMS (ESI, positive) *m/z* calcd for $C_{25}H_{26}O_9$ ($[M]^+$): 469.4740, found: 469.3763.

*4.1.3.3. 3-(2-acetyl-5-methoxyphenoxy) propyl cinnamate (compound **3**).*. Compound 2f replaced compounds 2d as material, others procedures as the same as compounds 1.

White crystal (EtOAc). m.p. 75–76 °C. Yield: 65%; ^{1}H NMR (400

Group B

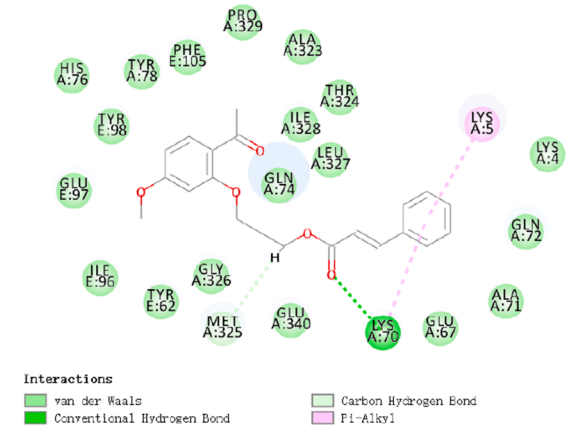

Compound 8

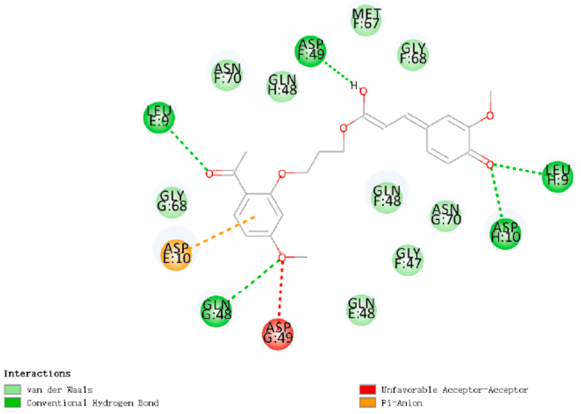

Compound 14

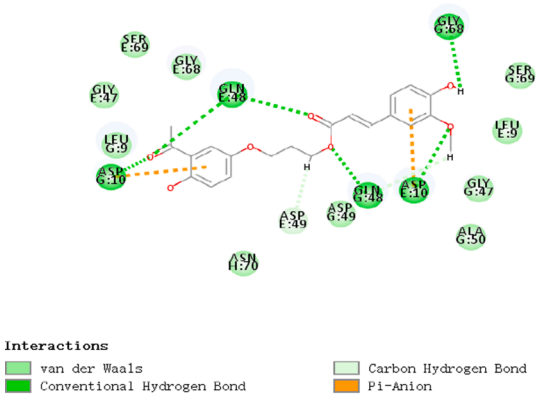

Compound 13

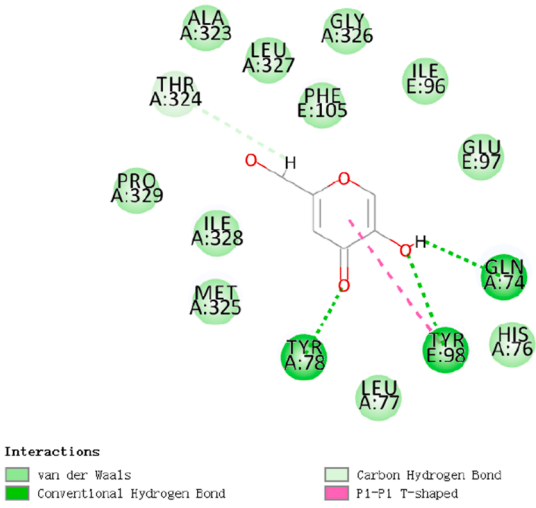

Kojic

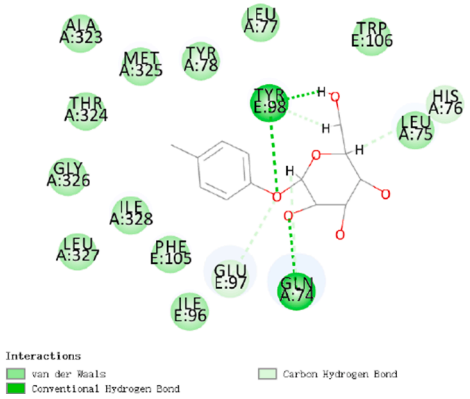

Arbutin

Fig. 9. (*continued*).

MHz, $CDCl_3$) δ 7.90 (d, $J = 10.4$ Hz, 1H), 7.70 (d, $J = 15.9$ Hz, 1H), 7.57 (d, $J = 31.1$ Hz, 2H), 7.41 (d, $J = 18.9$ Hz, 1H), 7.27 (s, 1H), 6.87 (s, 1H), 6.68 (d, $J = 18.2$ Hz, 2H), 4.42 (d, $J = 5.9$ Hz, 2H), 4.17 (d, $J = 5.9$ Hz, 1H), 2.40 – 2.15 (m, 2H), 1.60 (d, $J = 9.3$ Hz, 2H), 1.25 (s, 2H); ^{13}C NMR (100 MHz, $CDCl_3$) δ195.99, 167.03, 165.32, 162.99, 145.23, 134.09, 129.09, 128.56, 123.68, 116.90, 109.62, 65.05, 61.11, 29.70, 28.59; IR (cm^{-1}): 2941.43, 2890.54, 2364.27, 2327.87, 1968.56, 1642.92, 1603.43, 1564.35, 1415.99, 1258.56, 1206.17, 1058.54, 961.62, 832.27, 711.23, 613.01.HRMS (ESI, positive) *m/z* calcd for $C_{21}H_{22}O_5$ ($[M]^+$): 354.4020, found: 353.3917.

Table 3
The docking score of 1–14 compounds inhibitors with mushroom tyrosianse:

Compounds	Dock Score	Compounds	Dock Score
1	72.4421	12	61.7
2	83.1585	13	103.89
3	75.2711	14	97.34
4	85.2159	Ferulic	36.02
5	87.4696	Caffeic acid	37.38
6	75.0121	Cinnamic	55.14
7	90.6535	Paeonol	55.45
8	92.1343	Eugenol	58.29
9	58.9965	Kojic	52.01
10	86.4831	Arbutin	67.22
11	89.1886	2′,4′-Dihydroxyacetophenone	54.52

*4.1.3.4. (E)-3-(4-acetyl-3-hydroxyphenoxy) propyl 3-(4-acetoxy-3-methoxyphenyl) acrylate (compound **4**)*. Compound 1c replaced compounds 1a as material, others procedures as the same as compound 1.

White crystal. m.p. 143–144 °C. Yield: 65%; 1HNMR (400 MHz, CDCl3) δ12.74 (s, 1H), 7.66 (s, 1H), 7.64 (d, $J = 1.2$ Hz, 1H), 7.63(t, 1H), 7.17 (s, 1H), 7.13 (d, $J = 1.9$ Hz, 1H), 7.10 (dd, $J = 3.8$, 1.8 Hz, 2H), 7.06 (s, 1H), 7.04 (s, 1H), 6.45 (d, $J = 2.5$ Hz, 1H), 6.44 – 6.42 (m, 2H), 6.40 (s, 1H), 6.36 (s, 1H), 4.40 (t, $J = 6.2$ Hz, 2H), 4.14 (t, $J = 6.2$ Hz, 2H), 3.88 (s, 6H), 2.55 (s, 3H), 2.23(s, 3H), 2.19 – 2.16 (m, 2H); ^{13}CNMR (100 MHz, $CDCl_3$) δ202.77, 168.98, 166.86, 165.34, 165.28, 151.44, 141.51, 132.45, 121.40, 114.01, 108.15, 101.31, 64.80, 61.22, 55.99, 28.49, 26.39, 20.79; IR (cm^{-1}): 2962.35, 2889.58, 2359.82, 1757.29, 1715.34, 1632.21, 1509.73, 1377.54, 1327.59, 1253.68, 1189.7, 1170.32, 1160.73, 1063.45, 998.03, 844.99, 819.08, 598.06; HRMS (ESI, positive) *m/z* calcd for $C_{24}H_{24}O_8$ $[M]^+$: 428.4370, found: 427.4297.

*4.1.3.5. (E)-4-(3-(3-(4-acetyl-3-hydroxyphenoxy)propoxy)-3-oxoprop-1-en-1-yl)-1, 2-phenylene diacetate(compound **5**)*.. Compound 1c replaced compounds 1a as material, others procedures as the same as compounds 2. White crystal. m.p. 88–89 °C. Yield: 73%; ^{1}H NMR (400 MHz, $CDCl_3$) δ12.74 (s, 1H), 7.66 – 7.58 (m, 2H), 7.41 (d, $J = 2.1$ Hz, 1H), 7.39 (d, $J = 2.1$ Hz, 1H), 7.36 (d, $J = 2.1$ Hz, 1H), 7.23 (s, 2H), 7.22 (d, $J = 8.4$ Hz, 1H), 6.45 (d, $J = 2.5$ Hz, 1H), 6.43 (d, $J = 8.4$ Hz, 1H), 6.38 (d, $J = 8.4$ Hz, 1H), 4.39 (t, $J = 6.2$ Hz, 2H), 4.13 (t, $J = 6.2$ Hz, 2H), 2.56 (s, 3H), 2.32 – 2.29 (m, 6H), 2.25 – 2.16 (m, 2H), 1.57 (s, 2H); ^{13}C NMR (100 MHz, $CDCl_3$) δ 202.81, 168.30, 166.65, 165.34, 165.27, 143.26, 142.49, 132.48, 124.07, 119.01, 108.12, 101.35, 64.78, 61.33, 28.45, 26.35, 20.80, 20.76; IR (cm^{-1}) 3412.74, 3072.89, 2963.33, 2899.11, 2621.23, 1770.16, 1701.95, 1630.20, 1559.66, 1420.12, 1375.31, 1251.94, 1195.70, 1054.45, 998.21, 899.14, 827.47, 710.46, 601.39. ESI-MS: HRMS (ESI, positive) *m/z* calcd for $C_{24}H_{24}O_9$ ($[M]^+$): 456.4470, found: 455.4372.

4.1.3.6. (E)-4-(3-(3-(4-allyl-2-methoxyphenoxy) propoxy)-3-oxoprop-1-en-1-yl)-1, 2-phenylene diacetate (compound 6).. Compound 1b replaced compounds 1a as material, others procedures as the same as compounds 2.

White crystal (EtOAc).m.p. 74–75 °C. Yield: 60%; ^{1}H NMR (400 MHz, $CDCl_3$) δ 7.63 (d, $J = 16.0$ Hz, 1H), 7.41 (dd, $J = 8.5$ Hz, 1H), 7.39 (d, $J = 8.5$ Hz, 1H), 7.35 (d, $J = 16.0$ Hz, 1H), 7.22 (d, $J = 8.4$ Hz, 1H), 6.83 (d, $J = 8.4$ Hz, 1H), 6.71 (d, $J = 6.4$ Hz, 1H), 6.38 (d, $J = 6.4$ Hz, 1H), 5.95 (m, $J = 6.7$ Hz, 1H), 5.07 (t, $J = 14.5$ Hz, 1H), 4.17 (t, 2H), 3.82 (d, $J = 14.5$ Hz, 9H), 3.32 (s, 1H), 2.79 (s, 1H), 2.30 (s, 3H), 2.11 – 1.97 (m, 2H), 1.63(s, 2H), 1.25 – 1.22 (m, 2H); ^{13}C NMR (100 MHz, $CDCl_3$) δ 168.27, 168.20, 166.67, 146.56, 142.97, 137.74, 133.27, 120.50, 119.25, 115.78, 113.49, 112.34, 65.78, 61.74, 55.97, 39.93, 28.75, 20.81, 20.77; IR (cm^{-1}) 2941.43, 2890.54, 2364.27, 2327.87, 1968.56, 1642.92, 1603.43, 1564.35, 1415.99, 1258.56, 1206.17, 1058.54, 961.62, 832.27, 711.23, 613.01. HRMS (ESI, positive) *m/z* calcd for $C_{26}H_{28}O_8$ ($[M]^+$): 468.5020, found: 467.4419.

*4.1.3.7. (E)-3-(4-allyl-2-methoxyphenoxy) propyl 3-(4-acetoxy-3-methoxyphenyl) acrylate (compound **7**)*.. Compound 1b replaced compounds 1a as material, others procedures as the same as compounds 1.

White solid. m.p. 79–80 °C. Yield: 68%; ^{1}H NMR (400 MHz, $CDCl_3$) δ7.64 (d, $J = 16.0$ Hz, 1H), 7.26 (s, 1H), 7.10 (s, 2H), 7.05 (d, $J = 8.0$ Hz, 1H), 6.84 (d, $J = 8.0$ Hz, 1H), 6.71 (d, $J = 6.1$ Hz, 1H), 6.38 (d, $J = 16.0$ Hz, 1H), 5.95 (d, $J = 16.8$, 6.7 Hz, 1H), 5.08 (d, $J = 17.0$ Hz, 2H), 4.42 (t, $J = 5.1$ Hz, 2H), 4.14 (t, $J = 6.3$ Hz, 2H), 3.86 (d, $J = 7.8$ Hz,3H), 3.33 (d, $J = 6.7$ Hz, 1H), 2.24 (dd, $J = 8.1$, 4.5 Hz, 2H), 1.57(s, 1H); ^{13}C NMR (100 MHz, $CDCl_3$) δ168.97, 168.89,151.42, 149.51, 146.58, 144.21, 141.44, 137.73, 133.42, 133.30, 123.34, 120.49, 118.28, 115.79, 113.51, 112.38, 111.22, 65.82, 61.65, 55.99, 39.92, 28.78; IR(cm^{-1}) 2920.34, 2360.96, 1725.26, 1606.95, 1552.89, 1417.52, 1319.77, 1247.40, 1175.28, 1139.46, 1064.98, 995.54, 786.96, 710.54, 610.51. HRMS (ESI, positive) *m/z* calcd for $C_{25}H_{28}O_7$ $[M]^+$: 440. 4920, found: 439.4391.

*4.1.3.8. 3-(3-acetyl-4-hydroxyphenoxy) propyl cinnamate (compound **8**)*.. Compound 1c replaced compounds 1a as material, others procedures as the same as synthesis compounds 3.

White crystal (EtOAc/ petroleum ether).m.p: 117 °C; Yield: 64%; ^{1}H NMR (400 MHz, $CDCl_3$) δ 7.92–7.86 (dd, $J = 15.9$ Hz, 2H), 7.7 (d, $J = 12.0$ Hz, 1H), 7.6 (d, $J = 6.0$ Hz, 2H), 7.54–7.52 (s, $J = 6.0$ Hz, 2H), 7.43 (d, $J = 3.0$ Hz, 1H), 4.38 (t, $J = 12$ Hz, 2H), 4.13 (t, $J = 9.0$ Hz, 2H), 3.81 (s, 3H), 2.54 (s, 3H), 2.34 – 2.09 (m, 2H); ^{13}C NMR (100 MHz, $CDCl_3$) δ196.00, 167.03, 165.33, 162.9, 151.43, 147.77, 145.00, 134.37, 130.98, 129.01, 128.55, 117.85, 116.92, 112.46, 109.63, 65.04, 61.10, 29.70, 28.58; IR: 3414.76, 2910.35, 2360.96, 1720.21, 1606.95, 1552.89, 1415.66, 1319.77, 1247.40, 1175.28, 1138.83, 1062.98, 995.54, 766.96, 710.38, 620.15. ESI-MS: 339.38HRMS (ESI, positive) *m/z* calcd for $C_{20}H_{20}O_5$ ($[M]^+$): 340.3750, found: 339.3834.

*4.1.3.9. 3-(4-allyl-2-methoxyphenoxy) propyl cinnamate (compound **9**)*.. Compound 1c replaced compounds 1a as material, others procedures as the same as synthesis compounds 3.

White solid (EtOAc/ petroleum ether). m.p: 115 °C; Yield: 77%; ^{1}H NMR (400 MHz, $CDCl_3$) δ7.69 (d, $J = 16.0$ Hz, 1H), 7.53 (s, 2H), 7.39 (t, 2H), 6.85 (d, $J = 8.6$ Hz, 1H), 6.72 (s, 2H), 6.44 (d, $J = 16.0$ Hz, 1H), 5.95 (m, $J = 5.5$ Hz, 1H), 5.08 (d, $J = 18.6$ Hz, 2H), 4.42 (t, $J = 6.2$ Hz, 2H), 4.14 (t, $J = 6.3$ Hz, 2H), 3.85(s, 3H), 3.34 (d, $J = 6.6$ Hz, 2H), 2.30–2.19 (m,2H), 1.57 (s,1H); ^{13}C NMR (100 MHz, $CDCl_3$) δ196.84, 167.51, 165.05, 163.48, 152.23, 147.72, 145.67, 134.69, 132.14, 131.5, 130.92, 129.5, 128.4, 127.90, 124.81, 117.50, 116.93, 112.56, 61.05, 29.98. IR (cm^{-1}): 2966.26, 2359.96, 1771.99, 1706.48, 1629.35, 1554.31, 1417.05, 1249.95, 1228.36, 1009.59, 837.03, 813.41, 711.19, 608.22. HRMS (ESI, positive) *m/z* calcd for $C_{22}H_{24}O_4$ ($[M]^+$): 352.4300, found: 351.3562.

*4.1.3.10. (E)-3-(2-acetyl-5-methoxyphenoxy) propyl 3-(4-((tert-butyldimethylsilyl)oxy)-3- methoxyphenyl)acrylate (compound **10**)*.. The solution of acetic anhydride (25 mM, 10 eq) was added to a solution of compound 4 (1.5 mM, 1 eq) in DCM, and the mixture was refluxed for 2 h. $SOCl_2$ (0.15 M) was added to a solution of Compound2a (1.0 mM) in DCM (20 mL), and the mixture was refluxed for 5 h at 75 °C. Then the solution was heated to 85 °C for evaporation. After cooling to room temperature, and then concentrated under reduced pressure to obtain yellow solution, which went straight to the next reaction. Compounds 1a-c (2.5 mM, 1.7 eq) was added at 0 °C, and then added NEt_3 (5 mM, 2 eq). The reaction was stirred at room temperature overnight and monitored by TLC. The mixture was washed with water and brine respectively. The organic layer was dried over $MgSO_4$, and then concentrated under reduced pressure to give a bright yellow oil as an intermediate. The obtained residue was purified by silica gel chromatography using petroleum ether/ethyl acetate (1:1, v: v) as original eluent to give compounds 10–12 (Yield: 65–75%).

White crystal. m.p. 80–81 °C. ^{1}H NMR (400 MHz, $CDCl_3$) δ 7.85 (d, J = 8.8 Hz, 1H), 7.63 (d, J = 15.9 Hz, 1H), 7.26 (s, 1H), 7.03 (dd, J = 5.4, 2.0 Hz, 3H), 6.84 (d, J = 8.7 Hz, 1H), 6.53 (dd, J = 8.8, 2.3 Hz, 1H), 6.46 (d, J = 2.3 Hz, 1H), 6.29 (d, J = 15.9 Hz, 1H), 4.42 (t, J = 6.2 Hz, 2H), 4.18 (t, J = 6.2 Hz, 2H), 3.84 (d, J = 4.1 Hz, 8H), 2.61 (d, J = 2.5 Hz, 3H), 2.36 – 2.20 (m, 2H), 1.58 (d, J = 1.2 Hz, 1H), 1.01–0.95 (m, 9H); ^{13}C NMR (100 MHz, $CDCl_3$) δ 202.75, 167.30, 165.38, 165.30, 151.26, 147.69, 145.32, 132.43, 127.36, 123.00, 121.12, 115.46, 113.99, 110.76, 108.17, 101.31, 64.85, 60.96, 55.50, 28.55, 26.38, 25.73, 18.58; IR (cm^{-1}): 3891.33, 2855.73, 2362.10, 1700.70, 1610.32, 1552.48, 1415.97, 1272.62, 904.53, 842.09, 710.08. HRMS (ESI, positive) *m/z* calcd for $C_{27}H_{38}O_6Si$ ($[M]^+$): 498.6910, found: 497.6240.

4.1.3.11. (E)-3-(2-acetyl-5-methoxyphenoxy) propyl-3-(4-((tert-butyldimethylsilyl) oxy)-3-methoxyphenyl) acrylate (compound 11).. The compound 1c was replaced with the compounds 1a, others synthesis peocedures as the same as the synthesis of 10.

White crystal (EtOAc) m.p. 79–80 °C. Yield: 66%; ^{1}H NMR (400 MHz, $CDCl_3$) δ12.74 (s, 1H), 7.62 (s, 1H), 7.61 (d, 1H), 7.02 (s, 2H), 6.84 (d, J = 8.6 Hz, 1H), 6.45 (d, J = 8.5 Hz, 2H), 6.29 (d, J = 15.9 Hz, 1H), 4.39 (t, J = 6.2 Hz, 2H), 4.14 (t, J = 6.2 Hz, 2H), 3.83 (s, 3H), 2.55 (s, 3H), 2.27– 2.10 (m, 2H), 1.57(s, 2H), 0.99 (s, 9H); ^{13}C NMR (100 MHz, $CDCl_3$) δ173.23, 165.21, 132.37, 128.22, 122.48, 120.80, 115.46, 114.19, 111.31, 107.65, 100.64, 65.04, 60.98, 55.58, 26.31, 25.65; IR (cm^{-1}): 3238.39, 2944.03, 2891.54, 2855.82, 2622.35, 2359.74, 1701.44, 1608.34, 1553.95, 1416.34, 1272.61, 1152.55, 905.83, 842.02, 710.98, 612.37. HRMS (ESI, positive) *m/z* calcd for $C_{27}H_{36}O_6Si$ ($[M]^+$): 484.6640, found: 483.5265.

*4.1.3.12. (E)-3-(4-allyl-2-methoxyphenoxy) propyl −3-(4-((tert-butyldimethylsilyl)oxy)-3- methylphenyl)acrylate (compound **12**).*. The compound 1b was replaced with the compounds 1a, others synthesis peocedures as the same as the synthesis of 10.

White crystal (EtOAc). m.p. 155–156 °C. Yield: 61%; ^{1}H NMR (400 MHz, $CDCl_3$) δ12.54 (s, 1H) , 7.61 (d, J = 7.9 Hz, 1H), 7.41 (d, J = 2.0 Hz, 0H), 7.39 (d, J = 2.0 Hz, 1H), 7.36 (d, J = 1.9 Hz, 1H), 7.22 (d, J = 8.4 Hz, 1H), 4.39 (t, J = 6.2 Hz, 2H), 4.11 (t, J = 6.1 Hz, 2H), 3.86 (s, 3H), 2.54 (s, 3H), 2.31 (d, J = 2.5 Hz, 2H), 2.21 (s, 1H), 2.21 (s, 1H), 1.58 (s, 1H); ^{13}C NMR (100 MHz, $CDCl_3$) δ198.75, 165.39, 160.89, 132.41, 121.19, 106.45, 98.15, 66.89, 60.95, 55.76, 32.09, 31.31, 25.63; IR (cm^{-1}): 2861.34, 256.19, 1745.26, 1680.59, 1671.64, 1630.29, 1601.34, 1580.61, 850.32, 790.25, 751.38, 680.24. HRMS (ESI, positive) *m/z* calcd for $C_{29}H_{40}O_5Si$ ($[M]^+$): 496.7190, found: 495.7261.

*4.1.3.13. (E)-3-(2-acetyl-5-methoxyphenoxy) propyl-3-(4-hydroxy-3-methoxyphenyl) acrylate (compound **13**).*. 1 mL NH_4F of THF solution (1 mol/L, 1.5 eq) was added to a solution of the compound 11 (0.2 mmol, 1 eq) in THF (20.0 mL), and the mixture was stirred for 4 h at room temperature. The reaction mixture was concentrated, which was washed with saturated $NaHCO_3$, H_2O and brine respectively. The organic layer was dried with $MgSO_4$, which was purified by chromatography to give 13 as a pale yellow powder and white powder respecticely (Yield: 70.6%).

White powder (CH_3OH).m.p. 127–128 °C; Yield: 54%;^{1}H NMR (400 MHz, $CDCl_3$) δ12.79(s, 1H), 7.64 (s, 1H), 7.62 (d, J = 6.0 Hz, 1H), 7.08 (dd, J = 6.0 Hz, 2 Hz, 1H), 7.03 (d, 1H), 6.92 (s, J = 6.0 Hz, 1H), 6.46 (d, J = 3.0 Hz, 1H), 6.43 (d, J = 3.0 Hz, 1H),4.38 (t, J = 9.0 Hz, 2H), 4.13 (t, J = 9.0 Hz,2H), 3.92 (s, 3H),2.20 (m, J = 6.2 Hz, 2H), 2.55 (s, 3H); ^{13}C NMR (100 MHz, $CDCl_3$) δ195.96, 167.01, 165.29, 162.98, 151.50, 147.76, 134.36, 129.08, 128.55, 123.72, 117.84, 112.45, 109.63, 64.79, 61.10, 28.10, 26.50, 26.12, 20.68; IR (cm^{-1}) 3434.96, 3238.39, 2955.44, 2893.19, 2856.26, 1699.01, 1628.08, 1509.92, 1469.06, 1280.11, 1265.24, 1180.25, 1020.38, 903.50. HRMS (ESI, positive) *m/z* calcd for $C_{21}H_{22}O_7$ ($[M]^+$): 386.4000, found: 385.3173.

*4.1.3.14. (E)-3-(3-acetyl-4-hydroxyphenoxy) propyl −3-(4-hydroxy-3-methoxyphenyl) acrylate (compound **14**).*. 1 mL NH_4F of THF solution (1 mol/L, 1.5 eq) was added to a solution of the compound 10 (0.2 mmol, 1 eq) in THF (20.0 mL), other procedure were accordance with the synthesise of the compound 13. Product as white powder have gain eventually (Yield: 76%).

White powder (CH_3OH).m.p. 152–153 °C; Yield: 35%; ^{1}H NMR (400 MHz, CDCl3) δ12.76 (s, 1H), 7.65 (s, 1H), 7.62 (d, J = 1.0 Hz, 1H), 7.03 (m, J = 6.0 Hz, 2H), 6.84 (d, J = 8.2 Hz, 1H), 6.45 (d, J = 3 Hz, 1H), 6.44 (s,1H), 6.30 (d, 1H), 4.40 (d, J = 6.4 Hz, 2H), 4.15 (d, J = 6.3 Hz, 2H), 3.93 (s, 3H), 3.33 (s,3H), 2.70 – 2.48 (m, 2H), 2.19 (s, 3H), 2.04 (s, 1H), 1.31 – 1.21 (m, 2H); ^{13}C NMR (100 MHz, $CDCl_3$) δ197.63, 197.61, 194.74, 164.61, 164.60, 164.46, 133.25, 120.62, 105.07, 105.06, 105.03, 100.0, 99.04, 66.69, 55.65, 55.62, 32.01, 30.99; IR: 3585.91, 3414.30, 1653.24, 1630.48, 1582.63, 1430.25, 1120.56, 840.65, 730.28, 708.51, 620.65. HRMS (ESI, positive) *m/z* calcd for $C_{22}H_{24}O_7$ ($[M]^+$): 400.4270, found: 399.1528.

4.2. Tyrosinase activity assay

4.2.1. Anti-tyrosinase activity

The measurement of tyrosinase (EC 1.14.18.1) inhibition was possessed according to the method of Nazir with minor modification [46,47]. Mushroom tyrosinase (Sigma-aldrich, 1000 Umg^{-1}), L-3, 4-dihydroxyphenylalanine (L-dopa), dimethyl sulfoxide (DMSO) were purchased from Sigma Chemical Co (St. Louis, Mo, USA). All of compounds were dissolved in DMSO, which tested for di-phenolase inhibitory activity of tyrosinase by L-dopa as substrate.Thetest controls the final concentration of DMSO in the solution was 2.0%. Firstly, 160 μL of phosphate buffer (pH 6.86), 20 μL of mushroom tyrosinase (final concentration: 50U/mL^{-1}) and 10 μL of the inhibitor solution were combined in a centrifuge tube. After pre-incubation for 10 min at room temperature, 10 μL L-dopa (final concentration: 0.4 mM) was added to the mixture to examine immediately. The enzyme reaction was monitored for 1 min by measuring the change in absorbance at 475 nm corresponding to the formation of dopachrome. Inhibition of tyrosinase reaction was calculated as follows: inhibition ratio (I%) = $[(A_s\text{-}A_b)/(Ac\text{-}Ab)] \times 100$, where$A_b$ and A_s are the absorbance of the blank and samples.

4.2.2. Kinetic analysis of the inhibition of mushroom tyrosinase

A series of diluted inhibitor solutions were prepared (8: 0, 15, 31, 62 and 125 μM, 13: 0, 7, 15, 31, and 62 μM, 14: 0, 15, 31, 62 and 125 μM). The L-dopa concentration was 0.4 mM and the concentration of tyrosinase were 0.0, 8.3, 16.7 and 33.3 U mL^{-1}, respectively. Substrate L-dopa concentration range from 0.2 to 1.6 mM in all kinetic study. Pre-incubation and measurement time wasthe same as discussed in mushroom tyrosinase inhibition assay protocol. The formation of L-dopa chrome was continuously monitored at 475 nm for 5 min at a 30 s interval in the microplate reader after the addition of enzyme. Inhibition type on the enzyme was assayed by Lineweaver–Burk plots of inverse of velocities (1/V) versus inverse of substrate concentration 1/[S], and the inhibition constant $K_I$was determined by the Dixon plot of 1/V versus inhibitor concentrations.

4.2.3. Cytotoxicity of compounds 8, 13 and 14

$B_{16}F_{10}$ melanoma cell (1.5×10^5 cells/L) line obtained from (Cell Bank of the Chinese Academy of Science, China) was cultured at 37 °C under 5% CO_2 atmosphere and was used to determine the cytotoxicity. The $B_{16}F_{10}$ cells ($10^4 \times$ cells/well) were seeded in Dulbecco's modified Eagle's medium (DMEM) containing 100 IU/mL penicillin, and 100 μg/mL streptomycin, supplemented with 10% FBS, under 5% CO_2 humidified atmosphere at 37 °C. The cell viability assay was evaluated by the conversion of MTT method to a purple formazan precipitate as previously described. After 24 h, the various concentrations of compounds were subsequently added and incubated for 24 h. The survival rate was

calculated from plotted results using cells untreated by test compounds as reference with some slight modifications [48]

4.2.4. Determine the cellular melanin content;

Melanin content assay was performed to evaluate the inhibitory effect of compounds 8, 11, 13and 14 (25, 50, 100, and 200 μM) on melanogenesis using the standard method with slight modification [49]. Briefly, control group containing 1×10^5 cells per well, and treated group with 1×10^5 cells containing 1 μM α-MSH and various concentrations of compounds 8, 11, 13, 14, kojic and A(25, 50, 100, and 200 μM) for 48 h. The medium was removed and then 1% Triton X-100 mixed in 10 mM phosphate buffered saline was added. The mixture was frozen at − 80 °C and thawed at room temperature. A freshly substrate (2 mM L-dopa) was preparedand then added to the supernatant and incubated. The absorbance of each well was subsequently read at 475 nm.

$$\text{Melanincontent}(\%) = [(A_s - A_b)/(A_c - A_b)]100$$

The A_s,A_b and $A_c$were the absorbance of test compounds, the blank and control group respectively.

4.2.5. Determination of cellular tyrosinase activity:

Tyrosinase inhibition assays of cinnamyl-phenol ester derivatives 8, 11, 13 and 14 were performed as previously described with slight modification [50,51]. In brief, $B_{16}F_{10}$ cells were inoculated at 5×10^4 cells per well in 96-well plates and incubated for 24 h in a humidified 5% CO_2 atmosphere at 37 °C. The cells were then treated with α-MSH (1 μM) and kojic acid (25 μM) or α-MSH (1 μM) and compounds8, 11, 13 and 14 (0, 5, 10, or 25 μM) and re-cultured for 24 h under the same conditions. Cells were then washed with PBS buffer, lysed with lysis buffer (100 μL containing 1% Triton X-100 (5 μL), 0.1 mM PMSF (5 μL), and 50 mM PBS (pH 6.8, 90 μL), frozen at − 80 °C for 30 min, centrifuged at 12,000 rpm for 30 min at 4 °C, transferred to 96-well plates, treated with L-dopa (total volume 100 μL; 80 μL of supernatant and 20 μL of 10 mM L-dopa), and incubated for 30 min at 37 °C. Tyrosinase inhibitions were determined by measuring optical densities at 475 nm in a Tecan, Mannedorfmicroplate reader. The experiment was performed in triplicate.

Tyrosinase activity (I%) = $[(A_s\text{-}A_b)/ (A_c\text{-}A_b)] \times 100$

The A_s, A_b and $A_c$were the absorbance of test compounds, the blank and control group respectively.

4.2.6. The DPPH free radical scavenging activities of compound 8, 13 and 14

The compounds 8, 13 and 14 were measured using a previously reported method with slight modification [52]. 1, 1-diphenyl-2-picrylhydrazyl (DPPH) were used and Vitamin C (Vc) was used as a reference material for a positive control. Briefly, in 96 well-plates 2.00 mL of - sample solution including Vc at different concentration levels (1.000, 0.667, 0.444, 0.296, 0.198, 0.132, 0.0878, 0.059, 0.039 mmol/ L); compound 13 at different concentration levels (1.000, 0.667, 0.444, 0.296, 0.198, 0.132, 0.0878, 0.059 mmol/ L); Compound 8 and 14 at - different concentration levels (4.000, 2.683, 1.788, 1.19, 0.795, 0.530, 0.353 mmol/ L) was added to 2.00 mL of DPPH solution (0.268 mmol/ L in methanol solution). The reaction mixture was fully - shaken and incubated at 25 °C for 30 min in the dark, and then - the absorbance of the mixture solution was measured at 517 nm. The scavenging activity of DPPH free radical was calculated as following: DPPH radical scavenging activity (%) = $(A_0\text{-}A_1)/A_0 \times 100\%$. Where A_0 is the absorbance of DPPH solution without samples; A1 is the absorbance of DPPH with compound 8, 13, 14 or Vc .

4.2.7. Molecular docking

Molecular docking software was applied to further analyze the intrinsic interaction mechanism of ligand molecules and amino acid residues at the molecular level. The crystal structure of mushroom tyrosinase was retrieved from the RCSB DATE Bank (PDB:2Y9X). Ligand structures files were built with Discovery Studio 2019 software, and Ledock software was used for the docking. All the ligand and water atoms were removed. The copper ions in the active site were kept. Hydrogen atoms were auto-added by the protein prepared on Ledock software to obtain protein file format. The final conformation and psf topology file were extracted for docking. Ligand molecular files are performed screened and prepared through the rules of Lipiski five. The native ligand was re-docked to investigate the validity of the docking protocol. The docking site was considered using the position of the tyrosinase inhibitor and the radius active sites were set to −29.76;-10.28; −42.21 dimensions. In order to verify the results of docking, the known tyrosinase inhibitors, such as arbutin and kojic acid (KA) were also docked to the molecule. As the results present (Fig. 8), the docked conformation of tropolonewas well superposed to the conformation in the crystal structure (RSMD < 1.0A).

Declaration of Competing Interest

The authors declare that they have no known competing financial interests or personal relationships that could have appeared to influence the work reported in this paper.

Acknowledgements

The authors would like to thank Shaanxi Province Key Technologies R&D Program (S2017-ZDYF-YBXM-SF-0639), Shaanxi University of Chinese Medicine Innovative team (2019-YL12) and Shaanxi University of Chinese Medicine Program (303-123890013) for financial support of this work.

Appendix A. Supplementary material

Supplementary data to this article can be found online at https://doi.org/10.1016/j.bioorg.2020.104512.

References

[1] H. Claus, H. Decher, Bacterial tyrosinases, Syst. Appl. Microbiol. 29 (2006) 3–14.
[2] S.Y. Seo, Y.K. Sharma, N. Sharma, Mushroom tyrosinase: recent prospects, J. Agric. Food Chem. 51 (2003) 2837–2853.
[3] Y.J. Kim, H. Uyama, Tyrosinase inhibitors from natural and synthetic sources: structure, inhibition mechanism and perspective for the future, Cell Mol. Life Sci. 62 (2005) 1707–1723.
[4] T.S. Chang, An updated review of tyrosinase inhibitors, Int. J. Mol. Sci. 10 (2009) 2440–2475.
[5] C.A. Ramsden, P.A. Riley, Tyrosinase: the four oxidation states of the active site and their relevance to enzymatic activation, oxidation and inactivation, Bioorg. Med. Chem. 22 (2014) 2388–2395.
[6] Y. Matoba, T. Kumagai, A. Yamamoto, H. Yoshitsu, M. Sugiyama, Crystallographic Evidence That the Dinuclear Copper Center of Tyrosinase Is Flexible during Catalysis[J], J. Biol. Chem. 281 (13) (2006) 8981–8990.
[7] M. Brenner, V.J. Hearing, The protective role of melanin against UV damage in human skin, Photochem. Photobiol. 84 (2008) 539–549.
[8] C. Pacelli, R.A. Bryan, S. Onofri, L. Selbmann, I. Shuryak, E. Dadachova, Melanin is effective in protecting fast and slow growing fungi from various types of ionizing radiation, Environ. Microbiol. 19 (2017) 1612–1624.
[9] A.S. Elobeid, A. Kamal-Eldin, M.A.K. Abdelhalim, A.M. Haseeb, Pharmacological Properties of Melanin and its Function in Health, Basic Clin. Pharmacol. Toxicol. 120 (2017) 515–522.
[10] J. Xie, H.H. Dong, Y.Y. Yu, S.W. Cao, Inhibitory effect of synthetic aromatic heterocycle thiosemicarbazone derivatives on mushroom tyrosinase: Insights from fluorescence, ^{1}H NMR titration and molecular docking studies, Food Chem. 190 (2016) 709–716.
[11] T. Pillaiyar, M. Manickam, V. Nmasivayam, Skin whitening agents: medicinal chemistry perspective of tyrosinase inhibitors, J. Enzyme Inhib. Med. Chem. 32 (2017) 403–425.
[12] G. Cardinali, D. Kovacs, M. Picardo, Mechanisms underlying post-inflammatory hyperpigmentation: lessons from solar lentigo, Ann. Dermatol. Venereol. 139 (2012) 148–152.
[13] R.L. Mort, I.J. Jackson, E.E. Patton, Melanocytes and their diseases, Development 142 (2015) 620–632.
[14] M. Asanuma, I. Miyazaki, N. Ogawa, Dopamine- or L-DOPA-induced neurotoxicity: the role of dopamine quinone formation and tyrosinase in a model of Parkinson's disease, Neurotox. Res. 5 (2003) 165–176.

[15] N. Jucevičiūtė, I. Banaitytė, A. Vaitkus, R. Balnytė, Preclinical signs of Parkinson's disease: A possible association of Parkinson's disease with skin and hair features, Med. Hypotheses 127 (2019) 100–104.
[16] M. Asanuma, I. Miyazaki, S. Murakami, F.J. Diaz, N. Ogawa. Striatal astrocytes act as a reservoir for L-DOPA, PLoS One. 9(2014) e10.1371/journal.pone.0106362.
[17] S. Sari, B. Barut, A. Ozel, D. Şöhretoğlu, Tyrosinase inhibitory effects of Vinca major and its secondary metabolites: Enzyme kinetics and in silico inhibition model of the metabolites validated by pharmacophore modelling, Bioorg. Chem. e10.1016/j.bioorg.2019.103259 (92) (2019) 2019.
[18] L. Wang, J.Y. Oh, Y. U. Jayawardena, Y.J. J, B.M. Ryu. Anti-inflammatory and anti-melanogenesis activities of sulfated polysaccharides isolated from Hizikia fusiforme: Short communication, Int. J. Biol. Macromol., 142 (2019) 545-550.
[19] Y.H. Kuo, C.C. Chen, P.Y. Wu, C.S. Wu, P.J. Sung, C.T. Lin, H.M. Chiang, N-(4-methoxyphenyl) caffeamide-induced melanogenesis inhibition mechanisms, BMC Complement Altern. Med. 17 (2017) 71–79.
[20] F. Pintus, M.J. Matos, S. Vilar, G. Hripcsak, C. Varela, E. Uriarte, et al., New insights into highly potent tyrosinase inhibitors based on 3-heteroarylcoumarins: Anti-melanogenesis and antioxidant activities, and computational molecular modeling studies, Bioorg. Med. Chem. 25 (2017) 1687–1695.
[21] F. Liu-Smith, L.F. Meyskens, Molecular mechanisms of flavonoids in melanin synthesis and the potential for the prevention and treatment of melanoma[J], Mol. Nutr. Food Res. 6 (2016) 1264–1274.
[22] Z. Sheng, S. Ge, X. Xu, Y. Zhang, P.P. Wu, X.T. Xu, C. Li, D.G. Zhao, X.W. Tang, Design, synthesis and evaluation of cinnamic acid ester derivatives as mushroom tyrosinase inhibitors, Medchemcomm 9 (2018) 853–861.
[23] F. Pintus, M.J. Matos, S. Vilar, G. Hripcsak, C. Varela, L. Santana, F. Borges, R. Medda, A.D. Petrillo, B. Era, A. Fais, New insights into highly potent tyrosinase inhibitors based on 3-heteroarylcoumarins: Anti-melanogenesis and antioxidant activities, and computational molecular modeling studies, Bioorgan. Med. Chem. 25 (2017) 1687–1695.
[24] AS Z. Ashraf, M. Rafiq, H. Nadeem. Carvacrol derivatives as mushroom tyrosinase inhibitors; synthesis, kinetics mechanism and molecular docking studies[J]. PLoS One. 5 (2017, 12) e0178069.
[25] J.R. Arroo, S. Sari, B. Barut, Flavones as tyrosinase inhibitors: kinetic studies in vitro and in silico[J], Phytochem. Anal. 3 (2020) 314–321.
[26] W.M. Chai, M.Z. Lin, F.J. Song, Rifampicin as a novel tyrosinase inhibitor: Inhibitory activity and mechanism[J], Int. J. Biol. Macromol. 102 (2017) 425–430.
[27] Z. Zhao, G. Liu, Y. Meng, Synthesis and anti-tyrosinase mechanism of the substituted vanillyl cinnamate analogues[J], Bioorg. Chem. 93 (2019), e103316.
[28] M.L. Gonçalez, M.A. Corrêa, M. Chorilli, Skin delivery of kojic acid-loaded nanotechnology-based drug delivery systems for the treatment of skin aging[J], Biomed. Res. Int. 35 (2013) 271–276.
[29] A.C. Bresthnach, M. Nazzaro-Porro, S. Passi, Azelaic acid therapy in disorders of pigmentation[J], Clin. Dermatol. 7 (1989) 106–119.
[30] K. Mazurek, E. Pierzchala, Comparison of Efficacy of Products Containing Azelaic Acid in Melasma Treatment, J. Cosmet. Dermato. 15 (2016) 269–282.
[31] M. Funayama, H. Ararakawa, R. Yamamoto, Effects of alpha- and beta-arbutin on activity of tyrosinases from mushroom and mouse melanoma[J], Biosci. Biotechnol. Biochem. 59 (1995) 143–144.
[32] K.A. Arndt, T.B. Fitzpatrick, Topical use of hydroquinone as a depigmenting agent, Jama. 194 (1965) 965–967.
[33] M. Fan, G. Zhang, X. Hu, Quercetin as a tyrosinase inhibitor: Inhibitory activity, conformational change and mechanism[J], Food Res. Int. 100 (2017) 226–233.
[34] F. Pintus, J.M. Matos, S. Vilar, et al., New insights into highly potent tyrosinase inhibitors based on 3-heteroarylcoumarins: Anti-melanogenesis and antioxidant activities, and computational molecular modeling studies[J], Bioorgan. Med. Chem. 25 (2017) 1687–1695.
[35] M. Rafiq, Y. Nazir, Z. Ashraf, et al., Synthesis, computational studies, tyrosinase inhibitory kinetics and antimelanogenic activity of hydroxy substituted 2-[(4-acetylphenyl)amino]-2-oxoethyl derivatives[J], J. Enzyme Inhib. Med. Chem. 34 (2019) 1–11.
[36] S. Ullah, D. Kang, S. Lee, M. Ikram, C. Park, Y. Park, S. Yoon, P. Chun, H.R. Moon, Synthesis of cinnamic amide derivatives and their anti-melanogenic effect in alpha-MSH-stimulated B16F10 melanoma cells, Eur. J. Med. Chem. 161 (2019) 78–92.
[37] L.H. Peng, S. Liu, S.Y. Xu, L. Chen, Y.H. Shan, W. Wei, W.Q. Liang, J.Q. Gao, Inhibitory effects of salidroside and paeonol on tyrosinase activity and melanin synthesis in mouse B16F10 melanoma cells and ultraviolet B-induced pigmentation in guinea pig skin, Phytomedicine. 20 (2013) 1082–1087.
[38] J. Bu, P.C. Ma, Z.Q. Chen, W.Q. Zhou, Y.J. Fu, L.J. Li, C.R. Li, Inhibition of MITF and tyrosinase by paeonol-stimulated JNK/SAPK to reduction of phosphorylated CREB, Am. J. Chin. Med. 36 (2008) 245–263.
[39] J.L. Wang, G.Y. Wu, H.P. Chu, Z.Y. Wu, J.Y. Sun, Paeonol Derivatives and Pharmacological Activities: A Review of Recent Progress, Mini Rev. Med. Chem. 20 (2019) 466–482.
[40] X.N. Chen, L.P. Ren, M.L. Li, J. Qian, J.F. Fan, B. Du, Effects of clove essential oil and eugenol on quality and browning control of fresh-cut lettuce, Food Chem. 214 (2017) 432–439.
[41] A. Ali, Z. Ashraf, N. Kumar, M. Rafiq, F. Jabeen, J.H. Park, K.H. Choi, S.H. Lee, S. Y. Seo, E.H. Choi, P. Attri, Influence of plasma-activated compounds on melanogenesis and tyrosinase activity, Sci. Rep. 6 (2016) e10.1038/srep21779.
[42] Z. Sheng, S. Ge, X.M. Xu, Y. Zhang, P.P. Wu, K. Zhang, X.T. Xu, C. Li, D.G. Zhao, X. W. Tang, Correction: design, synthesis and evaluation of cinnamic acid ester derivatives as mushroom tyrosinase inhibitors, Medchemcomm. 9 (2018) 897.
[43] Z. Ashraf, D. Kim, S.Y. Seo, S.K. Kang, Synthesis and crystal structures of the potential tyrosinase inhibitors N-(4-acetylphenyl)-2-chloroacetamide and 2-(4-acetylanilino)-2-oxoethyl cinnamate, Acta Crystallogr. C Struct. Chem. 72 (2016) 94–98.
[44] Z. Ashraf, M. Rafiq, S.Y. Seo, M.M. Babar, N.S.S. Zaidi, Synthesis, kinetic mechanism and docking studies of vanillin derivatives as inhibitors of mushroom tyrosinase, Bioorg. Med. Chem. 23 (2015) 5870–5880.
[45] Q. Fan, H. Jiang, E.D. Yuan, J.X. Zhang, Z.X. Ning, S.J. Qi, Q.Y. Wei, Tyrosinase inhibitory effects and antioxidative activities of novel cinnamoyl amides with amino acid ester moiety, Food Chem. 134 (2012) 1081–1087.
[46] Y. Nazir, A. Saeed, M. Rafiq, S. Afzal, A. Ali, M. Latif, J. Zuegg, W.M. Hussein, C. Fercher, R.T. Barnard, M.A.T. Blaskovich, Z. Ashraf, Z.M. Ziora, Hydroxyl substituted benzoic acid/cinnamic acid derivatives: Tyrosinase inhibitory kinetics, anti-melanogenic activity and molecular docking studies, Bioorg. Med. Chem. Lett. 30 (2020) e 10.1016/j.bmcl.2019.126722.
[47] S. Ghafary, S. Ranjbar, B. Larijani, M. Amini, M. Biglar, M. Mahdavi, M. Bakhshaei, A. Sakhteman, Novel morpholine containing cinnamoyl amides as potent tyrosinase inhibitors, Int. J. Biol. Macromol. 135 (2019) 978–985.
[48] S. Lee, S. Ullah, C. Park, H.W. Lee, D.W. Kang, J. Yang, J. Akter, Y.J. Park, P. Chun, H.R. Moon, Inhibitory effects of N-(acryloyl)benzamide derivatives on tyrosinase and melanogenesis, Bioorg. Med. Chem. 27 (2019) 3929–3937.
[49] S. Ulaah, C. Park, M. Ikram, D. Kang, S. Lee, J. Yang, Y. Park, S. Yoon, P. Chun, H. R. Moon, Tyrosinase inhibition and anti-melanin generation effect of cinnamamide analogues, Bioorg. Chem. 87 (2019) 43–55.
[50] S. Ullah, Y. Park, M. Ikram, S. Lee, C. Park, D. Kang, J. Yang, J. Akter, S. Yoon, P. Chun, H.R. Moon, Design, synthesis and anti-melanogenic effect of cinnamamide derivatives, Bioorg. Med Chem. 26 (2018) 5672–5681.
[51] S. Ullah, D. Kang, S. Lee, M. Ikram, C. Park, Y. Park, S. Yoon, P. Chun, H.R. Moon, Synthesis of cinnamic amide derivatives and their anti-melanogenic effect in α-MSH-stimulated B16F10 melanoma cells, Eur. J. Med. Chem. 161 (2019) 78–92.
[52] M. Matos, C. Varela, S. Vilar, G. Hripcsak, F. Borges, L. Santana, E. Uriarte, A. Fais, A. Di Petrillo, F. Pintus, Design and discovery of tyrosinase inhibitors based on a coumarin scaffold, RSC Adv. 5 (2015) 94227–94235.